



# WPI

## Damage Detection in a Microencapsulated Dicyclopentadiene and Grubbs' Catalyst Self-Healing System

---

Major Qualifying Project completed in partial fulfillment  
of the Bachelors of Science Degree at  
Worcester Polytechnic Institute, Worcester, MA

Submitted by:  
Zhi Hao (Edward) Li  
Carly Morrison  
Elise St. Laurent

Professor Amy Peterson, Faculty Advisor

## Abstract

Self-healing polymers are able to repair themselves after being damaged. One type of self-healing system functions by microencapsulating a healing agent. Microcapsules were prepared to contain both a healing agent, dicyclopentadiene (DCPD), in addition to a damage detection agent, 1,3,5,7-Cyclooctatriene (COT). These microcapsules were incorporated into an epoxy matrix to create a damage detecting self-healing polymer. The DCPD-COT microcapsules were ruptured in the presence of Grubbs' catalyst, and color change was confirmed. Modified compact tension specimens were produced that contained DCPD and DCPD-COT microcapsules. Voids within the polymers as well as inhomogeneous incorporation of catalyst and microcapsules prevented the specimens from healing, so the effect of COT on the healing efficiency could not be tested. However, the addition of COT did not significantly impact the polymer's breaking strength.

## **Acknowledgements**

We would like to acknowledge Dr. Amy Peterson, our faculty advisor, Thomas Partington, machining specialist, Dr. Kathleen Field, and Claire Salvi, Anthony D'Amico, and Shubhneet Sandhu, our graduate student mentors.

## Table of Contents

Abstract .....	2
Acknowledgements .....	3
Table of Figures .....	6
1 Introduction .....	7
2 Background .....	8
2.1 Self-healing polymers .....	8
2.2 Chemistry of microcapsule-based self-healing polymers .....	9
2.3 Mechanical Properties .....	9
3 Literature Review .....	11
3.1 Self-Healing Process Using Microencapsulated Dicyclopentadiene .....	11
3.2 Production of Microencapsulated Dicyclopentadiene Self-Healing Polymers .....	12
3.3 Accommodating Fluorescent Dyes in Microcapsule-based Self-Healing Polymer Systems .....	13
3.4 Fluorescence in Alternative Healing Systems .....	15
3.5 Mechanical Testing for Healing Efficiency .....	16
4 Methodology .....	18
4.1 Microencapsulation Process .....	18
4.2 Grubbs' Catalyst Protection .....	18
4.3 Differential Scanning Calorimetry .....	18
4.4 Thermogravimetric Analysis .....	19
4.5 Testing Color Change .....	19
4.6 Production of Epoxy Bars .....	19
4.7 Production of Modified Compact Tension Specimens .....	20
4.8 Mechanical Testing .....	21
5 Results and Discussion .....	22
5.1 Microencapsulation .....	22
5.1.1 Scanning Electron Microscopy (SEM) Analysis .....	22
5.1.2 Thermogravimetric Analysis .....	24
5.2 Color Change Test .....	27
5.3 Production of Mechanical Testing Specimens .....	29

5.3.1 Differential Scanning Calorimetry Results .....	29
5.3.2 Microscope and SEM Images of the Specimens.....	35
5.3.3 Observations Made During Machining of the Specimens .....	38
5.4 Mechanical Testing .....	39
6.0 Conclusions and Recommendations .....	42
6.1 Conclusions.....	42
6.2 Recommendations.....	42
Appendix.....	44
Appendix A: Microencapsulation Procedure <sup>10</sup> .....	44
Appendix B: Grubbs' Protection Procedure <sup>21</sup> .....	44
References.....	45

## Table of Figures

Figure 2.1: Modified Compact Tension Specimen.....	9
Figure 3.1: Microcapsule Based Self-Healing.....	11
Figure 3.2: Tapered Double-Cantilever Beam Specimen.....	16
Figure 4.1: Specimen Dimensions.....	20
Figure 4.2: System for Loading Specimen.....	21
Figure 4.3: ElectroPuls with Specimen Holders.....	21
Figure 5.1: DCPD Microcapsule SEM Image.....	22
Figure 5.2: DCPD and COT Microcapsule SEM Image.....	23
Figure 5.3: Size Distribution of 198 DCPD Microcapsules.....	23
Figure 5.4: Size Distribution of 310 DCPD-COT Microcapsules.....	24
Figure 5.5: TGA of DCPD Microcapsules.....	25
Figure 5.6: TGA of DCPD-COT Microcapsules.....	26
Figure 5.7: TGA for Cure Cycle 1.....	27
Figure 5.8: TGA for Cure Cycle 2.....	27
Figure 5.9: Time-Lapse of DCPD-COT Microcapsule Color Test.....	28
Figure 5.10: Uncured Epoxy DSC Test Results.....	29
Figure 5.11: Determination of Enthalpy of Curing Reaction for Uncured Epoxy.....	30
Figure 5.12: Determination of $T_g$ for Uncured Epoxy.....	31
Figure 5.13: Cured Epoxy DSC Test Results.....	32
Figure 5.14: Determination of Enthalpy of the Curing Reaction for Cured Epoxy.....	33
Figure 5.15: Determination of $T_g$ for Cured Epoxy.....	34
Figure 5.16: SEM Image of Cab-o-sil Surface .....	36
Figure 5.17: SEM Image of Cab-o-sil Surface.....	36
Figure 5.18: Zeiss Image of Cab-o-sil Surface.....	37
Figure 5.19: Voids and Microcapsules near DCPD Sample Crack Surface.....	37
Figure 5.20: SEM Image of DCPD Crack Edge.....	38
Figure 5.21: Specimens D5 and C6 Before Testing.....	39
Figure 5.22: Loading of DCPD-COT Specimen.....	40
Figure 5.23: Breaking Force of Modified Compact Tension Specimens.....	41

## 1 Introduction

Self-healing polymers are able to repair themselves after damage to recover some or all of their original material properties. This ability enables prolonged use of the material after damage events, which is not possible in other polymers. Self-healing polymers are also able to heal autonomously, enabling the continued use of polymers after damage without the need for operators to take any action to repair the polymer.<sup>1</sup> Although self-healing capabilities can extend the lifetime of a polymer, these capabilities are limited by the method of self-healing that is used. Microcapsule-based self-healing polymers, for example, contain microencapsulated healing agents and are only capable of repairing a single damage event. Once the healing agent has reacted, it cannot heal damage at that site again, which means further damage will not be repaired. It is often hard to detect damage in polymers prior to a catastrophic event because of rapid crack propagation. As a result, the damage that self-healing systems are designed to heal is on the micro scale and it is often barely visible. This problem can be overcome by adding a means of detection to the self-healing polymer to visually distinguish a damaged site from the bulk polymer.<sup>2</sup> The application of self-healing systems will ultimately be in composite materials such as airplane wings or wind turbine. However, for research purposes it is easier to work with polymers without the composite additives.

Adding a detection agent to the healing agent is one method of allowing a healing site to become more visible. One possible detection agent is 1,3,5,7-Cyclooctatetraene (COT). COT polymerizes in the presence of Grubbs' catalyst, causing a color change but it is incapable of being used as the healing agent. If COT can be encapsulated with a healing agent, this can allow for a system with both healing and detection.<sup>3,4</sup> However, the addition of COT in microcapsule-based self-healing polymers also introduces complications since detection agents have the potential to affect material properties of the polymer. Detection agents may also interfere with the healing chemistry that takes place during damage. Therefore, research on the interaction between detection agents, bulk polymers, and encapsulated healing agents is valuable in determining how functional self-healing polymers with damage detection can be.<sup>5</sup>

The research questions this project will answer are:

- Does COT provide a means of detecting damage in a microencapsulated dicyclopentadiene (DCPD) and Grubbs' catalyst self-healing system?
- Does the use of COT as a detection agent affect the material properties of the microencapsulated DCPD and Grubbs' catalyst self-healing system?

We also attempted to determine whether the use of COT as a detection agent affects the fracture toughness healing efficiency of the microencapsulated DCPD and Grubbs' catalyst self-healing system.

## 2 Background

### 2.1 Self-healing polymers

Materials science focuses on improving performance of materials by widening materials' range of applications, quantifying material properties, and identifying failure mechanisms. Traditionally, materials have been engineered to prevent failure, but more recently, self-healing materials have taken a different approach. Instead of designing to prevent failure for as long as possible, the focus in self-healing materials is to facilitate recovery of the material's original properties. Using this self-healing approach by itself or in addition to traditional approaches is a promising area of materials engineering which opens up possibilities for improved materials.<sup>2</sup>

The three prevailing methods of self-healing materials are capsule-based, vascular, and intrinsic. These categories are defined by how healing agents are separated from the bulk matrix and have tradeoffs between number of healing cycles, bulk functionality after healing, and volume that can be healed.<sup>5</sup>

Capsule-based self-healing materials are materials whose healing agents are contained in capsules distributed in a bulk matrix. The capsules rupture to release healing agents when the bulk matrix is damaged. Consequently, the material loses its ability to heal when capsules are depleted due to a previous damage event. A few variations on capsule-based self-healing exist, but the more prevalent ones include capsule-catalyst and multi-capsule varieties. In capsule-catalyst, a catalyst is dispersed along with the healing agent capsules to facilitate the healing.<sup>6</sup> However, multi-capsules use multiple reactants that can be separately encapsulated, which are activated when mixed in the matrix during healing. Other less commonly used capsule-based self-healing variations include latent functionality in the bulk matrix and phase separation. Latent functionality is similar to capsule-catalyst, with the exception that the catalyst is unnecessary due to properties of the bulk. Phase separation refers to a variation that uses a minority phase in the bulk to separate healing agents.<sup>6</sup>

Vascular-based self-healing materials employ channels or capillaries to keep healing agents separate from the bulk. With connected gridding of healing agents, multiple healing events can occur at the same location until pathways become too blocked or healing agent is depleted.<sup>7</sup> Hollow glass fibers are commonly used because they are relatively unreactive and glass processing techniques already exist for other applications. Multiple isolated networks of vascular systems can be used to support two part healing chemistries or catalysts.<sup>7</sup> Structural health monitoring systems can also be incorporated within a vascular network by embedding carbon fiber laminates into a bulk polymer so that changes in resistance sensed by the laminate triggers an inherent local heating event. With a thermosetting epoxy, the heat promotes self-healing by initiating the epoxy chemistry and the epoxy is chosen to have a close solubility parameter to prevent phase separation.<sup>8</sup>

Intrinsic self-healing materials do not separate healing agents from a bulk because the self-healing mechanism depends on the intrinsic properties of these materials. They contain inherent reversibility of bonding, therefore only a limited number of materials can be used for intrinsic self-healing. Additionally, since most material properties are dependent on conditions the material is subjected to, such as temperature and pH, intrinsic self-healing materials have a limited range of



practicality compared to other self-healing options. Consequently, intrinsic self-healing is not as flexible when designing for a particular application. Polymers containing matrices with hydrogen bonding, thermoreversible bonding, or a dispersed thermoplastic phase are suited to intrinsic self-healing.<sup>9</sup>

## 2.2 Chemistry of microcapsule-based self-healing polymers

This project is focused on microcapsule-based self-healing polymers. The successful deployment of microcapsule-based self-healing polymers ultimately relies on two chemical processes: microcapsule formation and the reaction of the healing agent. Poly(urea-formaldehyde) will be used to encapsulate the healing agent dicyclopentadiene.

Poly(urea-formaldehyde) capsules are prepared in an oil and water emulsion under agitation.<sup>10</sup> During microencapsulation, urea and formaldehyde undergo a polymerization reaction at the oil-water boundary layer to form poly(urea-formaldehyde) and encapsulate the healing agent.<sup>11</sup> The polymerization reaction occurs in two steps: addition and condensation. During the addition reaction, urea reacts with formaldehyde to form monomethylol urea. Next, mono methylol urea condenses to form the polymer chain. This process then repeats to form the poly(urea-formaldehyde) polymer. See appendix for reaction diagrams.<sup>11</sup>

Dicyclopentadiene (DCPD) is a commonly used healing agent in self-healing polymers due to its ability to polymerize quickly with minimal shrinkage during healing, long shelf life, low viscosity, and low volatility.<sup>12</sup> DCPD polymerizes via ring opening metathesis polymerization (ROMP), which requires the use of a Grubbs' catalyst.<sup>5</sup> During ROMP, the double bond within the 6 carbon ring (Reaction 2.3) is broken and reformed with another broken double bond from a second DCPD monomer.<sup>13</sup> This process repeats, adding DCPD to the poly dicyclopentadiene chain. The newly formed poly(dicyclopentadiene) then fills damage sites and heals damage in the bulk polymer.

## 2.3 Mechanical Properties

Polymers and polymer composites are used for a variety of applications. They have been increasingly used in aircraft, cars, ships, and construction industries due to the high strength to weight ratios and tailorability of properties that they offer. However, polymers are also brittle and these applications require better material properties such as resistance to fracture, so that the polymers can be used to replace traditional materials. Self-healing polymers can help to improve durability as well as other material properties without the need for the damage to be detected. A common issue with polymer materials is microcracking, internal small cracks that can reduce the material's integrity. Crack propagation is also how material properties are weakened after impact and cyclic fatigue damage. Therefore, a common method of mechanical testing, especially for microcapsules systems, is fracture toughness.<sup>1</sup>

Fracture toughness is a measure of a material's resistance to fracture when it contains a crack. One method used in testing the fracture toughness a self-healing polymer is the modified compact tension test.<sup>14</sup> In this test, a specimen with the geometry shown in Figure 2.1 is subjected to a tensile loading stress. The specimen is notched and contains an arresting hole. Prior to testing,

a pre-crack is made in the notch of the specimen. The specimen is then loaded using dowels in the two holes shown in Figure 2.1. As the tensile load is increased, a crack is expected to form in the specimen propagating from the pre-crack and stopping at the arresting hole. The load at which this occurs can then be used to determine the fracture toughness of the polymer sample. The modified compact tension test is useful in measuring the properties of self-healing polymers because the geometry of the specimen produces a crack of consistent length, enabling the determination of the fracture toughness of the sample. Further, the geometry of the modified compact tension specimen is well suited for testing the healing properties of the polymer because the crack is not enabled to propagate through the entire polymer and the sample consequently remains in one piece after testing. This means that the crack surface is fixed in its alignment and is able to heal without the need for the surface to be aligned by human intervention.<sup>14</sup>

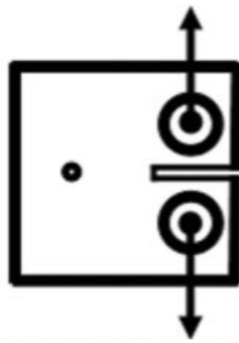


Figure 2.1: Modified Compact Tension Specimen<sup>14</sup>

Self-healing capabilities are needed to improve polymers as polymers become more widely used as a material. However, self-healing polymers are especially important because they can repair damage without the need for human intervention. If damage cannot be visually inspected or heard through a tap-test, then it is often costly to detect. In-depth inspection techniques include examination with ultrasonic devices, thermography, laser shearography, and laser interferometry. These methods all need technical equipment to detect damage, which is impractical in some situations and possible repair options can be costly.<sup>15</sup> A system that combines damage detection and self-healing properties would allow a material to keep its structural integrity until human intervention is able to take action.

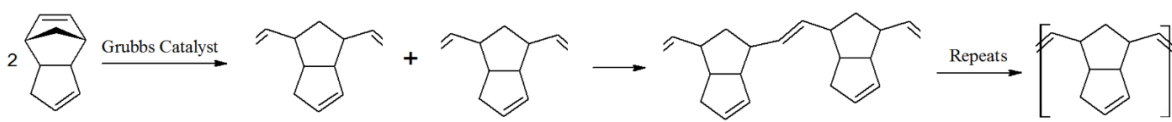
## 3 Literature Review

### 3.1 Self-Healing Process Using Microencapsulated Dicyclopentadiene

Dicyclopentadiene (DCPD) can be encapsulated and used as a healing agent. In order to polymerize DCPD, however, a Grubbs' catalyst must also be incorporated into the self-healing polymer as an additive. Grubbs' catalysts are metal carbene complexes.<sup>16</sup> In a metal carbene complex, the carbene complexes with a transition metal that can accept the carbene's lone pair using vacant d-orbitals.<sup>17</sup> In the Grubbs' catalyst, a ruthenium compound complexes with the carbene. The second and third generation Grubbs' catalysts are used for ring opening metathesis polymerization (ROMP).<sup>18</sup>

The Grubbs' catalyst serves to metathesize the functional groups of olefins across their double bonds, as shown in Reaction 3.1.<sup>16</sup>

Reaction 3.1 – ROMP Process



During olefin metathesis, the double bond of two olefins are severed. One severed double bond half of the first olefin then reacts with one of the severed double bond halves of the second olefin to form a new compound. The products of olefin metathesis can be any stereochemical combination of pairings between the double bond halves. ROMP is a specific type of olefin metathesis in which the double bond is within the ring of an aromatic compound. When the double bond of the ring is broken, the ring opens. Each severed double bond half is then reformed into a double bond with the severed double bond half of another opened ring, joining the carbon chains of the former rings together. This process repeats, creating the carbon chain that makes up the new polymer, poly(DCPD). The ROMP process for DCPD is shown in the appendix.

When a microencapsulated DCPD-based self-healing polymer is damaged and the microcapsules at the damage site rupture, DCPD is released from the microcapsules and undergoes ROMP using the Grubbs' catalyst embedded within the polymer.<sup>12</sup> The newly formed poly(DCPD) then serves to repair the damaged area by replacing the damaged bulk polymer. This process is illustrated in Figure 3.1

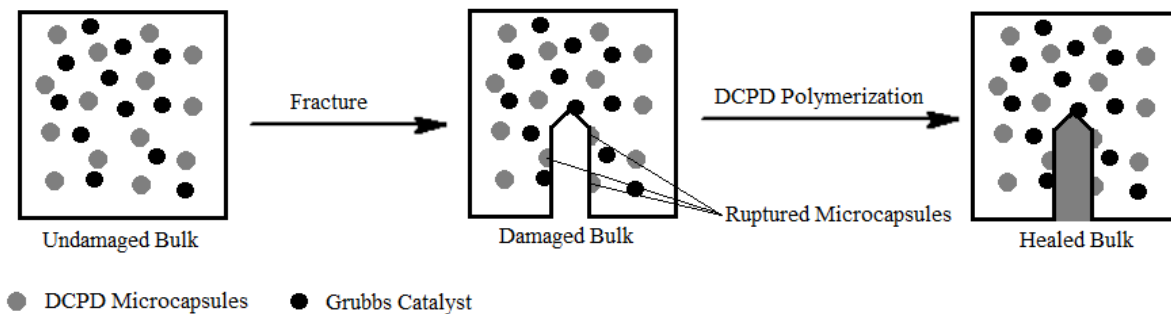


Figure 3.1: Microcapsule-based Self-Healing

### 3.2 Production of Microencapsulated Dicyclopentadiene Self-Healing Polymers

To form the microcapsules, it is essential that an oil and water emulsion is created. This allows the poly(urea-formaldehyde) (PUF) to encapsulate the oil phase, where the healing agent resides.<sup>10</sup> A mixture of ethylene-maleic anhydride copolymer (the oil phase) and deionized water are mixed under agitation then urea, ammonium chloride, and resorcinol are added to the solution, and the pH of the solution is adjusted to 3.5.<sup>10</sup> DCPD is then added to the solution and the solution is re-emulsified under agitation.<sup>10,19</sup> The agitation rate can be used to control the size of these droplets, which determine the size of the microcapsules.<sup>10</sup> Formaldehyde is added to the mixture and polymerizes to form PUF at the oil-water boundary layer.<sup>20</sup> After the reaction has run to completion, which can take several hours, the solution is cooled.<sup>10,19</sup> The microcapsules can then be separated from the solution through filtration, rinsed with deionized water, and air dried.<sup>10</sup> Grubbs' catalyst is very sensitive to air and it needs to be protected before adding it to an epoxy system. This can be done by encapsulating it in paraffin wax through a similar emulsion procedure to the microencapsulation.<sup>21</sup>

The microcapsules and Grubbs' catalyst are added to the polymer. The polymer is a cured epoxy resin, which is a thermosetting polymer. An epoxy is a compound containing a three-membered ring with an oxygen atom outside the main carbon chain.<sup>22</sup> When an epoxy reacts with a curing agent, such as an amine, the three-membered ring is broken and the curing agent and epoxy react to form a highly cross-linked thermosetting polymer. This high degree of cross-linking produces a thermosetting polymer with high toughness and mechanical strength, desirable thermal and electrical qualities, and high corrosion resistance.<sup>22</sup>

Commercial thermosetting polymers typically contain several additives intended to improve their properties. For example, anti-oxidizing agents can be added to thermosets to improve their resistance to oxidative degradation, fillers can be added to improve the cost or mechanical properties of thermosets, and surfactants can be added to improve the dispersion of other additives within the thermoset.<sup>23</sup> Since additives are widely used in thermosetting polymers, their effects and the procedure for adding them are generally well understood. In epoxy resin thermosets, these additives are added to the epoxy before curing takes place.<sup>19</sup> In DCPD based self-healing polymers, the microcapsules and Grubbs' catalyst are dispersed in the epoxy before curing takes

place. Homogenous dispersion is achieved with a planetary mixer. The epoxy mixture is poured into a mold and then cured in an oven.

Self-healing polymers can also be used in composite applications.<sup>5</sup> Glass fiber or carbon fiber reinforced self-healing polymer composites exhibit improved mechanical properties and could be used in a wider range of applications than self-healing polymers. However, when using standard ceramic composite material, only the thermosetting polymer phase would possess self-healing characteristics. Any damage that affected the ceramic composite material would be irreparable and material properties of the self-healing polymer composite would only be partially recoverable. Self-healing polymer composites can be produced through open molding by dispersing the microcapsules and Grubbs' catalyst within the epoxy, dispersing the ceramic composite material in the epoxy, and then curing the epoxy in a mold of the desired shape. However, in the case of self-healing polymers special care must be taken to avoid rupturing the microcapsules when dispersing the ceramic composite material in the epoxy.

### 3.3 Accommodating Fluorescent Dyes in Microcapsule-based Self-Healing Polymer Systems

Microcapsule-based self-healing is dependent on capsules used to release healing agents. Therefore, a given location within a bulk matrix is unable to heal repeatedly since capsules will be depleted by the first healing. Healing extends the life time of the polymer but after a healing event, the lifetime of the polymer in that area is limited as if it were an unmodified polymer. Fluorescent dyes encapsulated along with healing agents can be used to address this concern since depleted areas are highlighted by released dye. Self-healing materials which incorporate encapsulated dye can be visually inspected, providing a higher level of reliability when deciding whether or not to replace the part in service.

DCPD healing agent chemistries and PUF encapsulation described in Sections 3.1 and 3.2 are prevailing methods of self-healing in the literature, making fluorescent dyes compatible with these systems convenient. DCPD and other ROMP compatible compounds have been successfully encapsulated alongside fluorescent dye derivatives of 4,4'-diamino-2,2'-stilbenedisulfonic acid.<sup>24</sup> Noh and Lee<sup>25</sup> have shown by scanning electron and fluorescent microscope observations that this method of combining self-healing chemistries with fluorescent indicators is possible. However, there is a fundamental lack of understand of how fluorescent dyes affect degree of polymerization in ROMP based healing agent chemistries, healing efficiencies, and properties of material after healing.

Early methods of introducing visibility to damage sites in microcapsule-based self-healing polymers included addition of dyes to previously researched microcapsule. However, many of these early attempts ran into issues of compatibility with fluorescent dye and microcapsule material. Microcapsule synthesis is sensitive to any small changes in the core material such as adding a dye, manufacturing procedures involved with order of operation, ratio of reagents, and conditions of reaction.<sup>26</sup> As a result, papers describing the success of adding dye based damage indicators are mostly concerned with explaining their experimental studies to determine microcapsule recipes that adequately hold the core material. Literature has focused more on

ensuring that damaged sites fluoresce, with less concern given to how much the damaged sites fluoresce. More focus is put into improving the microcapsule that surrounds the healing agent and dye combination. Furthermore, there are secondary concerns noted by Li and associates<sup>27</sup> of restrictions due to weak adhesion of microcapsules to the bulk matrix, which reduces the original fracture toughness and tensile strength of the self-healing polymer. The introduction of dye based damage detection and all of its advantages in this study came at the cost of reduced original material properties.

More favorable fluorescent dyes would incorporate visual detection methods while also facilitating the healing process. Ideal detection mechanisms would also express immediate color change that transitions over time to show the act of healing. One system that has the potential to meet both of these goals incorporates the healing agent 1,3,5,7-Cyclooctatetraene (COT) with a Grubbs-Love catalyst. These additives have potential compatibility with DCPD, which could improve the healing process, while allowing detection.<sup>3,4</sup>

Finding a suitable recipe for capsules that would contain the COT healing agent and Grubbs-Love catalyst presented as much of a challenge for Odom et al. as choosing the healing agent and catalyst.<sup>3,4</sup> NMR spectroscopy was performed before and after breaking capsules with a mortar and pestle to determine if COT degraded inside capsules. Thermogravimetric analysis (TGA) was performed to determine thermal stability of microcapsules to ensure shell walls would survive. These results showed that capsules lose some small quantity of material even below the degradation temperature of capsules. Extensive experiments were performed on different encapsulation recipes to avoid premature color change from ruptured capsules. A final microcapsule recipe using COT as a core material was described as containing double the amount of urea and formaldehyde to produce microcapsules with much thicker shell walls.<sup>3,4</sup>

Pyrene has potential to be a damage indicator in microcapsule-based self-healing polymers that use a healing agent, such as DCPD, that reacts with a catalyst to undergo ROMP. Pyrene and its derivatives are already commercially used to manufacture dyes that function as molecular probes under fluorescence spectroscopy.<sup>28</sup> Turro and Arora<sup>29</sup> have used pyrene to observe interactions of water-soluble polymers in dilute solutions to take advantage of sensitivity of pyrene to the polarity of neighboring compounds that make up its environment. DCPD and poly(DCPD) both have low solubility in water so it is likely that pyrene will not fluoresce as brightly as it does in other pyrene applications.<sup>30</sup> However, pyrene is still a candidate as a damage indicator because even a small amount of fluorescence would provide enhanced damage visibility. Another possible way to incorporate pyrene as a damage indicator is to attach pyrene groups onto norbornene, since norbornene can participate in ROMP. These pyrene derivatives have been used successfully in biological fluorescence detection applications and norbornene healing agent chemistries have been previously studied.<sup>31</sup>

Pyrene must be encapsulated before it is useful in microcapsule-based self-healing polymers. Pyrene should be able to be encapsulated in the same way that DCPD is encapsulated described in Section 3.2 because pyrene is five orders of magnitude more soluble in oil than it is

in water.<sup>32</sup> A variation of the recipes used for DCPD may need to be used because microcapsules can be very sensitive to the materials which they are encapsulating.

Fluorescent dyes have been used within the field of self-healing polymer microcapsules outside of assessing serviceability of a bulk polymer after damage. Alternatively, fluorescent dyes can be used to gauge the integrity of the microcapsules. McIlroy et al. used Rhodamine B successfully as a fluorescent dye to gauge performance of amine filled microcapsules. This fluorescent dye was used to gauge the microcapsules integrity because encapsulation is usually dependent on emulsions between water and oil phases but amines are reactive in water, therefore this encapsulation has been difficult to achieve.<sup>33</sup> Perylene fluorescent dye was also used by the same research group to observe core material of binary microcapsules with liquid phases separated by Pickering stabilizers.<sup>31</sup> Although the primary purpose of Rhodamine B and perylene fluorescent dye was to assess microcapsule integrity, both also have potential to be used as fluorescent dyes for detection of damage sites.

### 3.4 Fluorescence in Alternative Healing Systems

Damage visibility is important for self-healing systems other than those based on microcapsules. Pang and Bond<sup>2</sup> incorporated visual indicators into their vascular self-healing system. Specifically, they were interested in introducing a UV fluorescent dye into a hollow fiber polymer composite matrix. The fluorescent dye used was Ardrex 985, and it was an effective damage detection agent. The point of the study was to detect low velocity impact damage, which can weaken structural integrity but is hard to detect. From their research, it is clear that the UV fluorescent dye worked effectively for damage detection under a UV light. However, the UV fluorescent dye did not indicate whether the site has been fully healed. These findings were also substantiated by ultrasonic C-scans, which are able to detect fractures in polymers. The hollow fiber system had healing efficiencies of 93%, but the effectiveness of the healing decreased with longer storage because acetone in the system caused the epoxy to degrade over time.

Other dyes have also been used in self-healing hollow fiber polymer matrices. One interesting additive that worked well was an X-ray opaque dye, di-iodomethane. Bleay et al.<sup>34</sup> combined the dye with the healing agent and filled the hollow fiber tubes using capillary action and a vacuum. The hollow fiber tubes were embedded in a polymer matrix and X-radiographs were taken that confirmed that dye was distributed in the tubes. Impact damage was inflicted on the polymer composite and new images were taken. These X-radiograph images clearly showed a concentration of the X-ray dye at the impact damage site. Klinga and Czigány<sup>35</sup> used Rhodamine B, another dye that has been effective when added to a self-healing agent. They found that using a UV lamp was the most effective way to quickly visualize the damage. Since they used hollow fibers, it was necessary to color the outside of the polymer matrix so that the undamaged section would not fluoresce as well.

There are a wide variety of systems that exhibit mechanochromic behavior, which is the ability to react visibly to damage from a mechanical force.<sup>36, 37, 38</sup> Most of these systems have not been tested with self-healing agents, but they show that other mechanisms are available for damage detection. An area of interest includes adding proteins with fluorescent characteristics into



polymers. One article describes combining chaperones from an organism with other proteins into a complex that exhibits fluorescence resonance energy transfer (FRET) when subjected to structural deformation. The mechanical stress causes the complex to separate and emit fluorescence.<sup>36</sup> Another article incorporates an enhanced yellow fluorescent protein (eYFP) at the glass fiber and polymer interface in a composite material.<sup>37</sup> An additional method for damage detection is a shift in color. Lowe and Weder<sup>38</sup> add excimers into a polymer blend. When the excimers are aggregated, which can be induced, they produce a red shift under UV light. After deformation, the excimers are dispersed producing a blue color under UV light. These articles represent just a small collection of the possible ways to improve damage detection using mechanochromic systems. Research on mechanochromic behavior is a thriving area because of the importance of damage detection in polymers and polymer composites.

### 3.5 Mechanical Testing for Healing Efficiency

Adding a detection agent to a self-healing system can affect the polymer's healing efficiency. Healing efficiency is a ratio of the mechanical properties of a polymer where healing has occurred to that of the original polymer. There are a variety of methods for examining the mechanical properties of self-healing polymers. These test methods include fracture toughness, compression, and a three or four point bend test.

For microcapsule-based self-healing polymers, fracture toughness has been the property that is most frequently tested. Often fracture toughness is tested using a tapered double-cantilever beam specimen. Fracture toughness is a measure of a material's resistance to fracture when it contains a crack. The test involves making a pre-crack then applying a load until the specimen breaks. Since only the load has to be determined and no crack lengths have to be measured, it is a relative easy test to run.<sup>39</sup> However, the tapered double-cantilever beam specimen is a very specific shape, as seen in Figure 3.2, and is hard to mold.

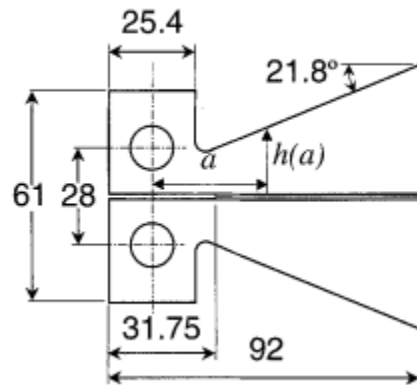


Figure 3.2: Tapered Double-Cantilever Beam Specimen<sup>19</sup>

The modified compact tension test can also be used to measure fracture toughness and determine healing efficiency.<sup>14</sup> The geometry used for the specimen in this test is shown in Figure 2.1 in Section 2.3. The specimen undergoes tensile loading until a crack forms in the specimen and



propagates from the pre-crack located in the notch of the specimen to the arresting hole. The specimen is then left to heal under high or low pressure conditions and retested in the same way. Like the tapered double-cantilever beam test, the healing efficiency of the modified compact tension specimen can be determined using the peak load of the specimen before and after healing, making this method of testing a simple way of determining healing efficiency. This method also has the advantage of using a specimen geometry that remains in one piece after fracture, and can heal without the need for human intervention to realign the crack surface, reducing the possibility for error.<sup>14</sup>

## 4 Methodology

In order to meet the objectives of this project, a set of microcapsules containing the healing agent dicyclopentadiene (DCPD) and another set of microcapsules containing both DCPD and 1,3,5,7-cyclooctatetraene (COT) were prepared. The DCPD-COT microcapsules were tested by damaging them and then monitored them for color change. After it was confirmed that the samples could undergo color change, the microcapsules were incorporated into epoxy test specimens along with the Grubbs' catalyst. The specimens were tested in order to determine the effect that the healing and detection agents had on the mechanical properties of the polymer.

### 4.1 Microencapsulation Process

Microcapsules were prepared in solution following the procedure adapted from Brown et al. which is available in Appendix A.<sup>10</sup> During the microencapsulation process, a stir rate of 550 rpm was used. One set of microcapsules contained DCPD and another set of microcapsules contained DCPD and COT. For the DCPD-COT microcapsules, the procedure from Brown et al. was modified by replacing the 30 mL of DCPD with 20 mL of DCPD and 10 mL of COT. This formulation was developed taking into account the procedures of Odom et al. for COT<sup>3,4</sup> encapsulation and White et al. using a smaller proportion of DCPD in their self-healing system.<sup>12</sup> The microcapsules were separated from the solution using vacuum filtration. They were allowed to dry on the filter paper for 24 hours in a fume hood before storing them in glass vials. The microcapsules were stored in the vials up to three weeks prior to using them in the production of the self-healing epoxy bars.

### 4.2 Grubbs' Catalyst Protection

Second generation Grubbs' catalyst was used as the catalyst for the polymerization of DCPD and COT. The Grubbs' catalyst was protected by coating it in wax. The purpose of coating the Grubbs' catalyst was to ensure that the catalyst was not deactivated by either exposure to air or by the amine used to cure the epoxy during the production of the epoxy bars.<sup>21</sup> Prior to coating, 0.5 g Grubbs' catalyst was enclosed in a vial with 9.6 g of paraffin wax in a glove box. The vials were left in the glove box under refrigerated conditions until the coating procedure. Two vials, or 1 gram of catalyst, were prepared in this way. The Grubbs' catalyst was encapsulated according to the procedure used by Rule et al., which is available in Appendix B.<sup>21</sup> The resultant wax-coated particles were separated from the solution using vacuum filtration. The wax-coated Grubbs' catalyst was dried on filter paper in a room temperature vacuum oven for three hours before storing it in vials. The protected catalyst was stored in the vials up to two weeks prior to using them in the production of the self-healing epoxy bars.

### 4.3 Differential Scanning Calorimetry

Differential scanning calorimetry (DSC) was performed on uncured epoxy and cured epoxy, so that information about the percent cure of the specimen bars could be determined. The uncured sample was taken before pouring uncured epoxy into the bar mold. The cured sample was

prepared by grinding down a chip of the epoxy bar with a mortar and pestle to yield a solid sample. Samples were loaded into pans before the sample pans were cold welded to a lid. Masses of pans, lids, and samples were each recorded as required input for the instrument. A 52.4 mg reference pan made up of a lid and a Concavus Pan Al cold welded together was used on both DSC runs. Both samples were subjected to a ramp from room temperature up to 250 °C, ramped down to -50 °C, and then ramped up to 250 °C all at 10 °C/min. The DSC was performed on a Netzsch 214 Polyma instrument.

#### 4.4 Thermogravimetric Analysis

Microcapsules were subjected to Thermogravimetric Analysis (TGA) using a Netzsch 209 F1 Libra. TGA was used to evaluate the success of microencapsulation and to examine the effects of the epoxy bar curing process on the microcapsules. Conclusions drawn from the TGA experiments were used to evaluate success of microencapsulation and were supplemented by Scanning Electron Microscopy (SEM) of microcapsule samples.

TGA was used to evaluate the success of the microencapsulation. Microcapsules were loaded into the crucible and subjected to heating from 30 °C to a plateau of 130 °C for 45 minutes before being heated again to 600 °C at heating rates of 10 °C/min. A mortar and pestle were used to prepare crushed capsules which were subjected to the same time and temperature profile for comparison.

Additionally, TGA was used to measure survival of microcapsules during epoxy bar curing process by applying the same conditions that were used in curing. Microcapsules were heated at heating rates of 10 °C/min from 30 °C to a plateau of 120 °C for two hours and then ramped up to a 140 °C plateau for another two hours. After observing a significant mass loss in the initial TGA used to examine effects of epoxy bar curing process on microcapsules, another TGA was performed with lower plateau temperatures. A subsequent TGA set to examine survival of microcapsules during epoxy bar curing process subjected of microcapsules loaded into the crucible to a ramp from 30 °C to a plateau of 100 °C for two hours before another ramp to a plateau of 120 °C for two more hours.

#### 4.5 Testing Color Change

A color change test was performed before making the epoxy bars. In this test, 87.5 milligrams of microcapsules and 9.4 milligrams of wax protected Grubb's catalyst were placed in the center of a microscope slide. Another microscope slide was placed on top, and the two slides were pushed together to ensure the rupture of microcapsules. Pictures were taken of the slide at zero hours, one hour, and seventeen hours.

#### 4.6 Production of Epoxy Bars

Two epoxy bars were prepared for mechanical testing, one with DCPD microcapsules and the other with DCPD-COT microcapsules. The epoxy bars were produced by mixing bisphenol A diglycidyl ether (DGEBA), as the epoxy resin, and bis-(p-aminocyclohexyl) methane (PACM), as the amine curing agent. These materials were mixed at 2000 rpm for two minutes and de-foamed

at 2200 rpm for thirty seconds in a planetary mixer. The test epoxy bars were prepared to contain microcapsules, Grubbs' catalyst, and Cab-o-sil. One weight percent Cab-o-sil was included to help with dispersion. The Cab-o-sil was combined with the epoxy and curing agent at the high speed mixing. Per 100 mL epoxy (approximately 116g), 3.7 grams of dried microcapsules and 0.4 grams of Grubbs' catalyst, which equaled 8.08 grams of wax protected Grubbs' catalyst, were used for each epoxy bar.<sup>3,4,19,39</sup> These amounts were chosen based on ratios used in Odom et al.' research.<sup>3,4</sup> The ratio of microcapsule to epoxy and Grubbs' catalyst to microcapsules fell within the optimal range of Brown et al.' research on microcapsule and catalyst loading.<sup>39</sup> The microcapsules and Grubbs' catalyst were mixed at a lower rate to prevent damage and microcapsule rupture. They were mixed at 200 rpm for two minutes and de-foamed at 220 rpm for thirty seconds. Around 50 mL of epoxy was made for each bar and this was poured into a mold. The epoxy was placed in an oven for two hours at 100°C and then two hours at 120°C.

#### 4.7 Production of Modified Compact Tension Specimens

Epoxy bars were processed through a series of machining steps to yield modified compact tension specimens for fracture toughness measurements (Figure 4.1). Whole epoxy bars were first milled down to the appropriate 14 mm width and 4 mm height dimensions. The bar was then cut with a band saw into sample pieces which were then milled down to 15 mm lengths.

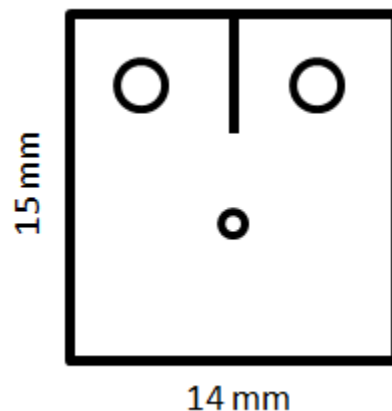


Figure 4.1: Specimen Dimensions

Using a drill press and premade drill press jig, appropriate holes were drilled into each specimen. The crack arresting hole required a #30/31 drill bit. The dowel holes on either side of where pre-crack would be made were drilled with a #60 bit. Some of the dowel holes could not easily accommodate the dowel meant to go through it. When this was the case, dowel holes were drilled out again or reamed out with the dowel until the dowel could be more easily inserted. A 'pecking' technique was used to drill out these holes. This technique involved drilling out a little bit of epoxy at a time to prevent epoxy shavings from interfering with the drilling in deeper segments of the hole. In between pecks, shavings were brushed off of the sample, jig, and drill bit.

A 6mm long notch with 1/32 inch width was cut into each. A modified band saw used to achieve this notch width. A premade saw jig was used for consistency across each sample.

Since epoxy bars containing DCPD and COT created an odor as capsules ruptured during machining, personal protective equipment was used. In addition to the safety goggles worn for machining, face masks and gloves were used to handle these bars.

#### 4.8 Mechanical Testing

Mechanical testing was performed to determine if adding the detection agent affects either the mechanical properties or the healing efficiency of the system. A system of dowels and collet was created for holding the test specimen in the ElectroPuls, Figure 4.2. A picture of the ElectroPuls can be seen in Figure 4.3.



Figure 4.2: System for Loading Specimen

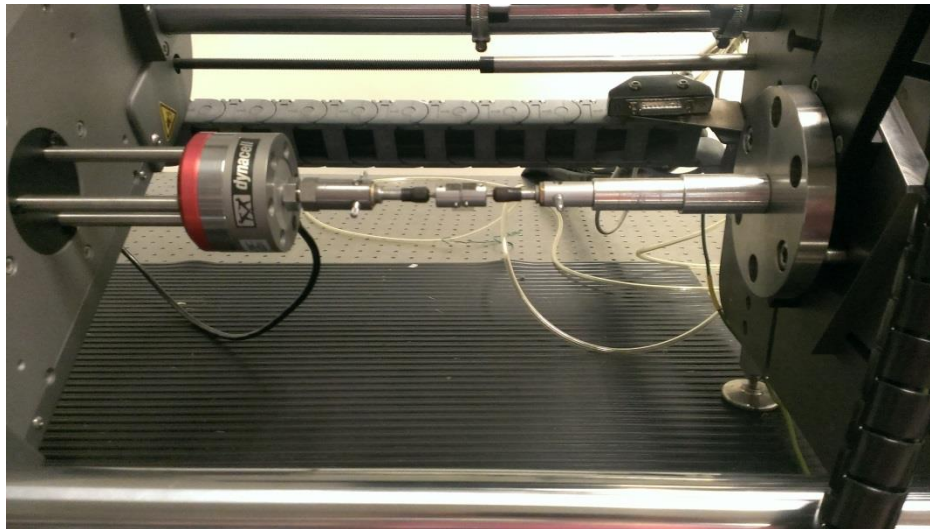


Figure 4.3: ElectroPuls with Specimen Holders

Specimens were loaded into the ElectroPuls and software was set up to track the force being applied at a loading rate of 0.1mm/min until the specimen broke

## 5 Results and Discussion

### 5.1 Microencapsulation

#### 5.1.1 Scanning Electron Microscopy (SEM) Analysis

After microencapsulation, Scanning Electron Microscopy was used (SEM) to evaluate size distributions of a DCPD microcapsule system (Figure 5.1) as well as a DCPD-COT microcapsule system (Figure 5.2). The difference in sample sizes of microcapsules in each microcapsule system is due to differences in preparation of each sample, but it is the size distribution that is worth characterizing.

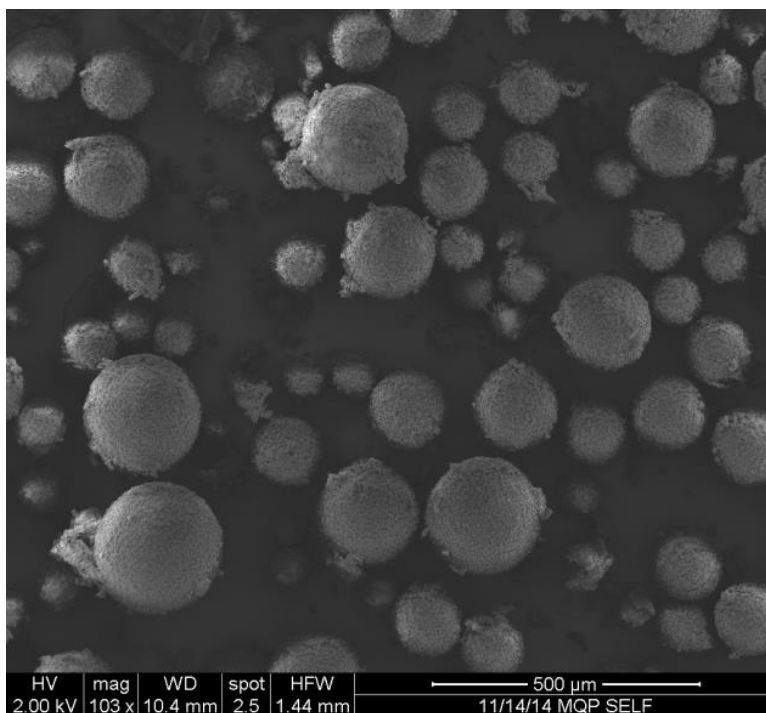


Figure 5.1: DCPD Microcapsule SEM Image

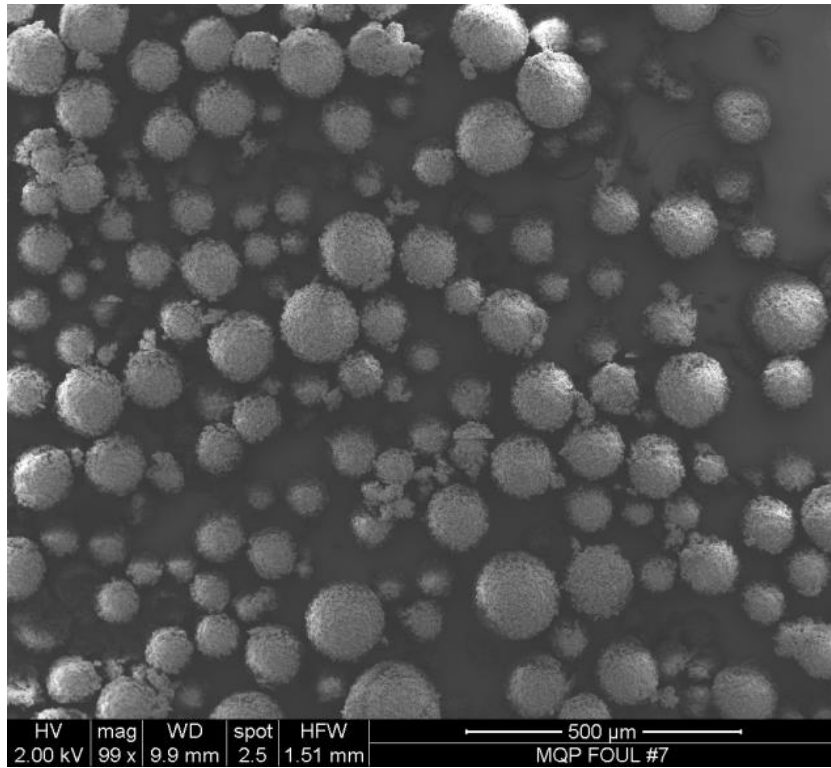


Figure 5.2: DCPD and COT Microcapsule SEM Image

During the DCPD microcapsule size distribution analysis, Figure 5.3, microcapsules were observed with a diameter range 61-230 $\mu$ m and an average diameter of 128 $\mu$ m across a sample size of 198 microcapsules. The average diameter is towards the low end of the range and 59.2% of the microcapsules in the sample size fell under the average diameter.

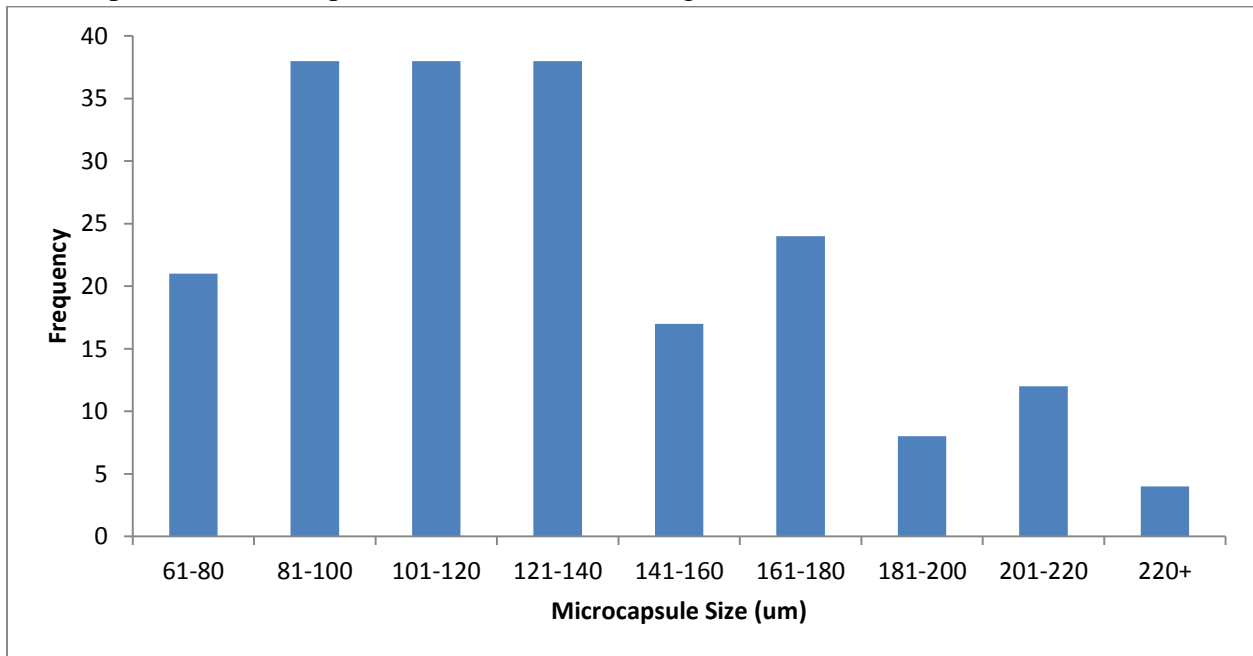


Figure 5.3: Size Distribution of 198 DCPD Microcapsules



During the DCPD-COT microcapsule size distribution analysis, microcapsules were observed with diameters ranging from 40-230 $\mu\text{m}$ , Figure 5.4. Out of the sample size of 310 capsules, 56.3% have diameters which are below the 99 $\mu\text{m}$  average. The average diameter is closer to the low end of the range.

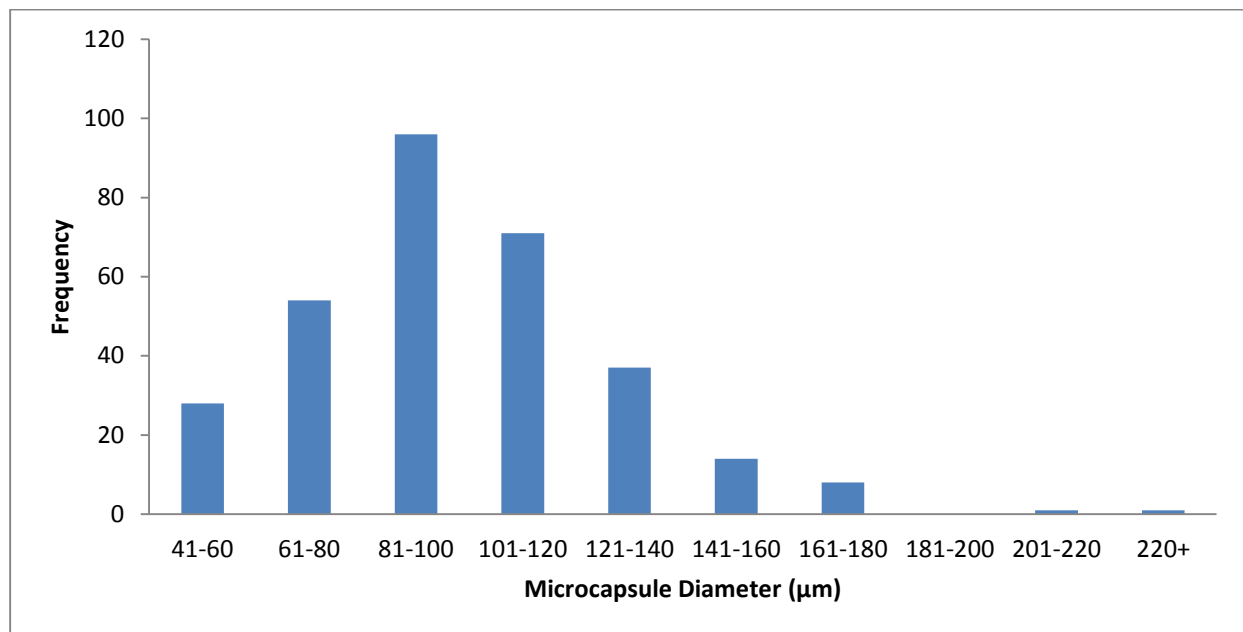


Figure 5.4: Size Distribution of 310 DCPD-COT Microcapsules

Both microcapsule systems have average diameters towards the low ends of their respective ranges. Furthermore, a microcapsule is more likely to have a smaller than average diameter. These observations suggest that larger microcapsules vary more widely in size and are less prevalent in the system.

Microcapsules with diameters between 161-230 $\mu\text{m}$  were arbitrarily characterized as large. Across both systems, 24.2% of the DCPD microcapsules and 7.7% of the DCPD-COT microcapsules fall under this category. This information suggests that COT microcapsules are in general smaller than DCPD microcapsules.

### 5.1.2 Thermogravimetric Analysis

Two thermogravimetric analyses (TGA) were performed on the microcapsules. The first was performed to discern how successful the microencapsulation was, and the second was performed to see how well microcapsules survived the curing process for the epoxy bar.

The success of the microencapsulation can be determined by understanding how much of the healing agent was encapsulated.<sup>40</sup> This was achieved by performing TGA analysis on a small sample of microcapsules. The microcapsules were heated as described in Section 4.4.

Figure 5.5 shows the results of the TGA for DCPD. A sharp dip occurs at 150  $^{\circ}\text{C}$ . It is believed that this dip corresponds to the rupture of the microcapsules, which should occur around



the boiling point of DCPD (170 °C with stabilizer). The mass lost before this sharp dip is considered to result from the loss of material that had not been encapsulated. To analyze the change in mass percent during the TGA, mass loss is calculated as a percent of the mass that is lost before versus the mass lost during the degradation of the microcapsules. Approximately 7.5% of the initial mass was burned off before the degradation of the microcapsules. The dip marking the degradation of the microcapsules resulted in an 88% mass loss. It can therefore be concluded the over 90% of the DCPD was encapsulated.

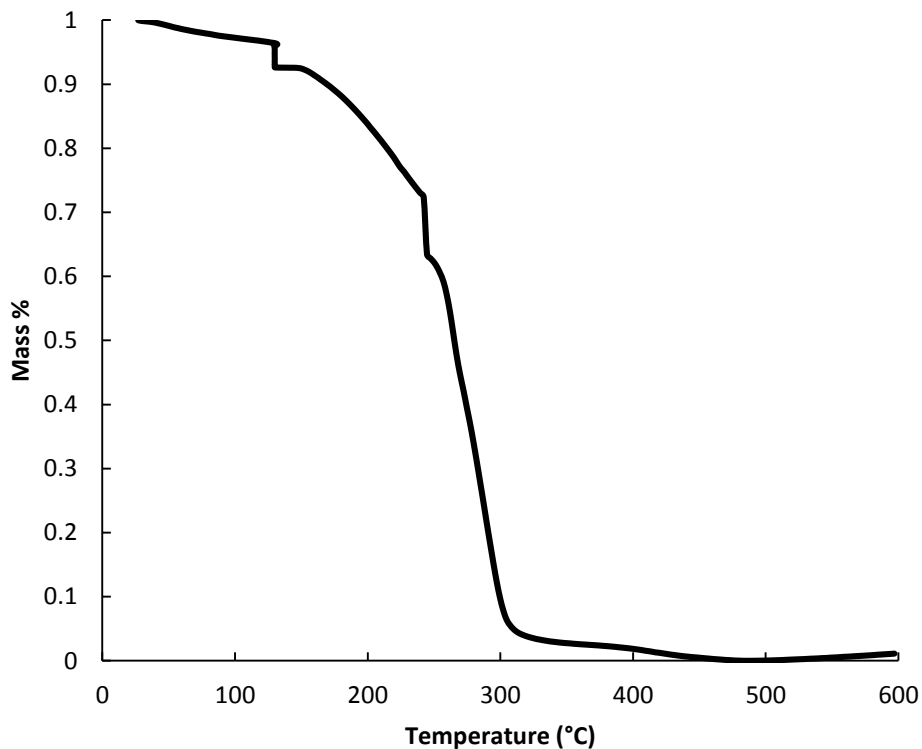


Figure 5.5: TGA of DCPD Microcapsules

Figure 5.6 shows the TGA for the DCPD-COT microcapsules. This microencapsulation was even more successful than the DCPD. Only 2% is lost before degradation and over 91% after the sharp dip, corresponding to 97% of the DCPD-COT was encapsulated.

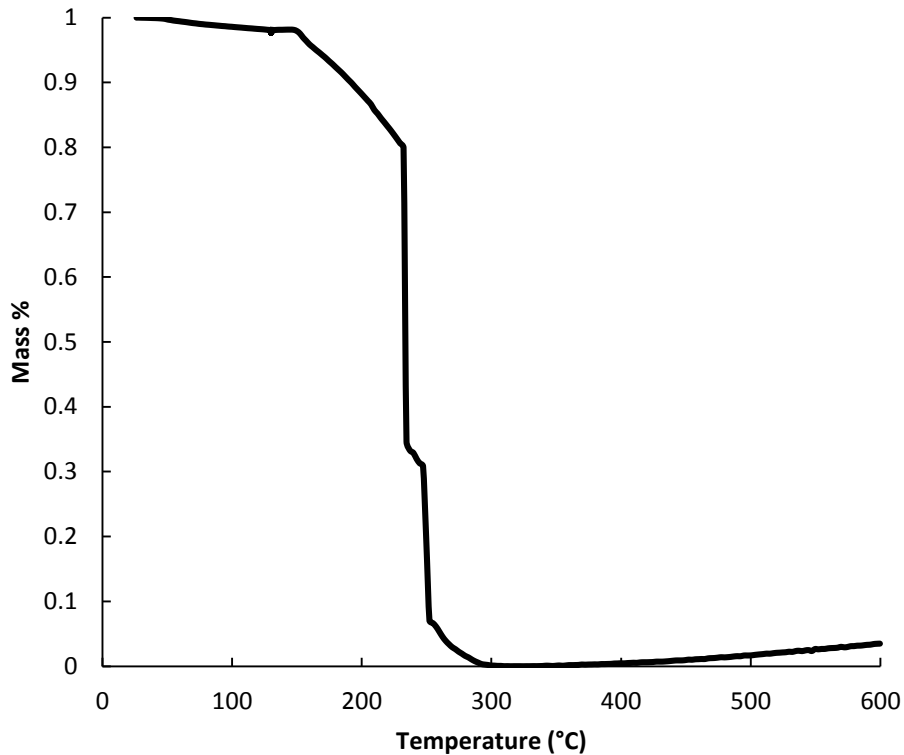


Figure 5.6: TGA of DCPD-COT Microcapsules

TGA was also used to determine how well microcapsules endure the cure cycle. This was tested by subjecting the microcapsules through the cure cycle temperatures over appropriate time intervals and seeing how much mass was lost. First, the cure cycle of 120°C for two hours and 140°C for two hours was tested, Figure 5.7. This resulted in approximately 15% of the mass being lost, likely through capsule rupture. The boiling point of DCPD with stabilizer is well over the temperatures<sup>40</sup>, so it is suspected that the poly(urea-formaldehyde) degraded at these temperatures. To prevent this mass loss during the production of the test bars, the cure cycle was reduced to 100 °C for two hours and 120 °C for two hours. The data for this cure cycle can be seen in Figure 5.8. The mass loss from this cure cycle was only 3%, therefore this is the temperature regime that was used for the epoxy bars.

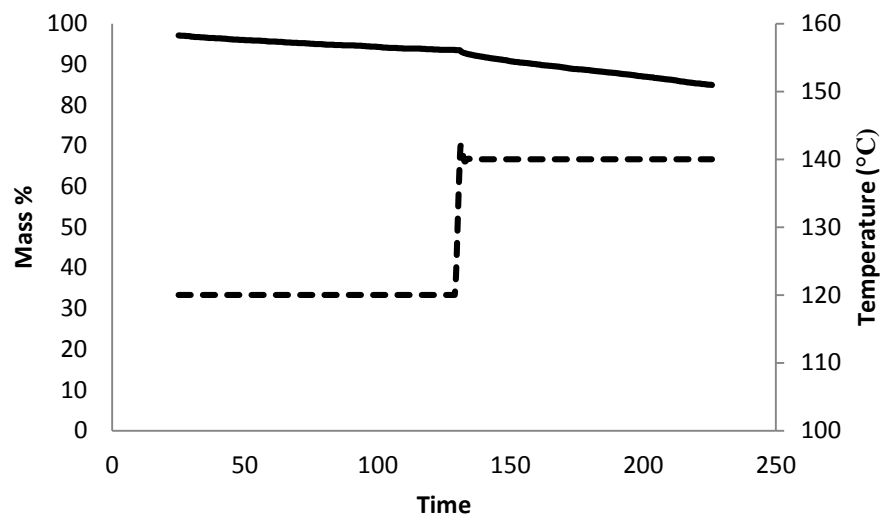


Figure 5.7: TGA for Cure Cycle 1

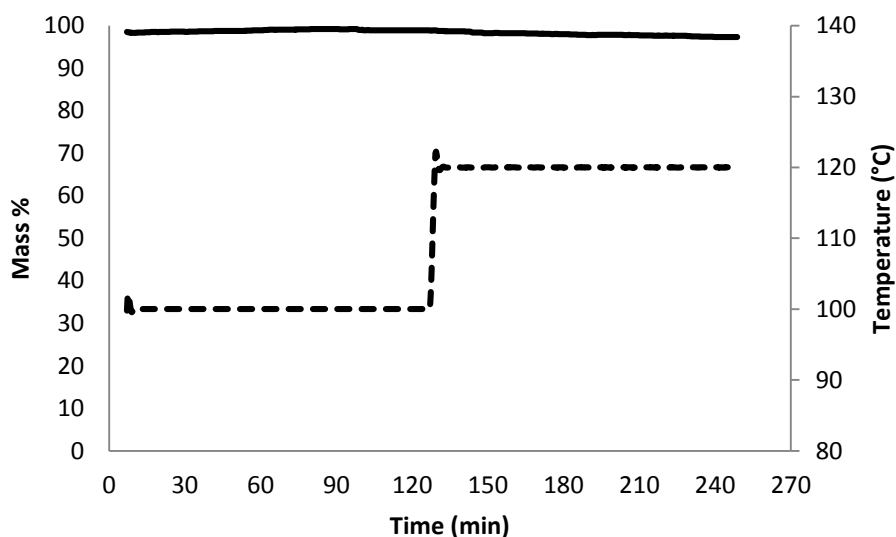


Figure 5.8: TGA for Cure Cycle 2

## 5.2 Color Change Test

Before adding the microcapsules and Grubbs' catalyst to the epoxy bars, the viability of the color change system was tested. The DCPD-COT microcapsules were added to the Grubbs' catalyst on a microscope slide. Another slide was then placed on top of the first slide and pushed down to crush the microcapsules. The following pictures in Figure 5.9 convey this color change over time.

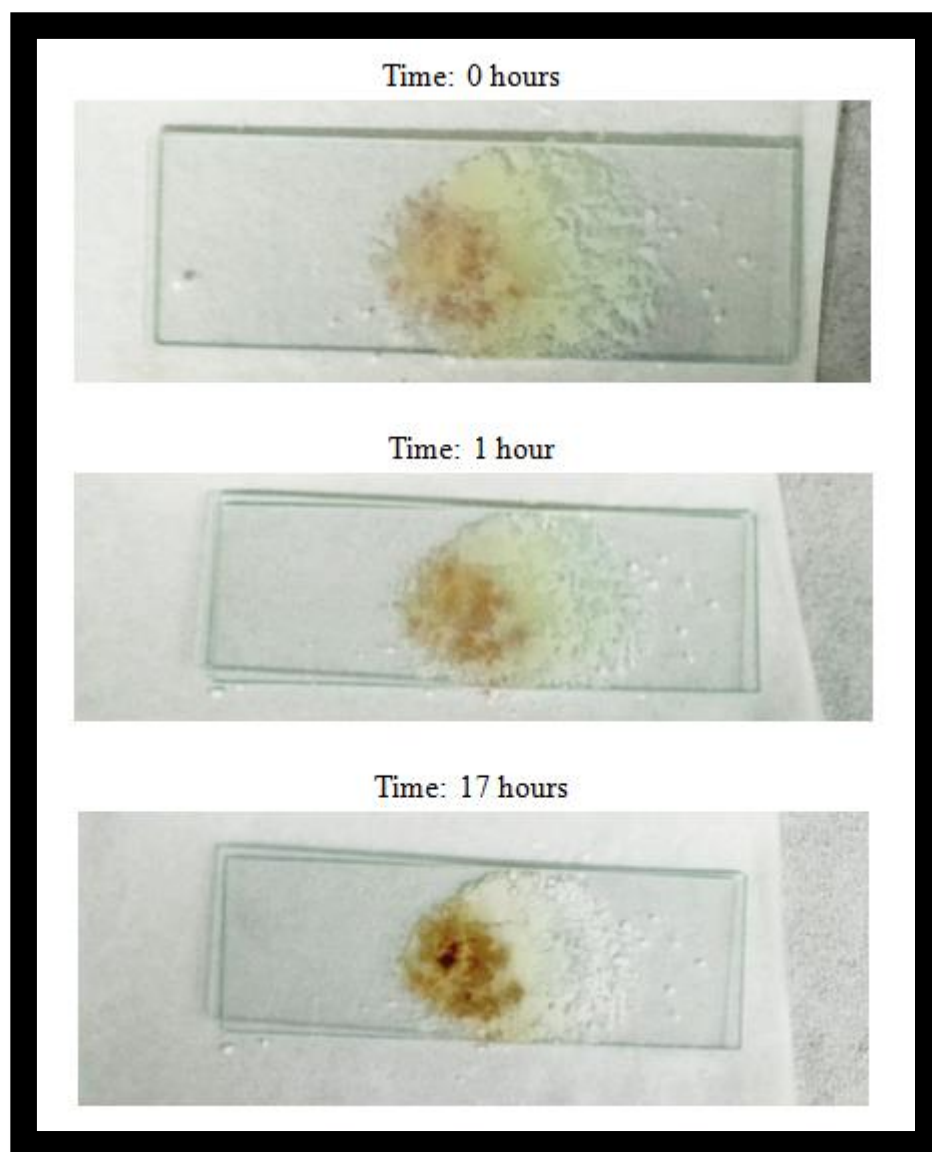


Figure 5.9: Time-Lapse of DCPD-COT Microcapsule Color Test

An immediate reaction at zero hours is not seen in the slide. However, liquid between the slides could be seen, confirming that the microcapsules had been crushed. After one hour, the first hint of a color change can be seen as the edges of the color spot seem to turn orange. The change is more noticeable after 17 hours. The color is a more vibrant orange and in the center a purplish color can be seen. From these pictures, it can be concluded that a color change occurred from the COT reacting with the Grubbs' catalyst.

A key goal of this project was to determine if the inclusion of COT in the microcapsule system would inhibit the functionality of DCPD or vice versa. The test confirms that the presence

of DCPD in the microcapsules did not prevent COT from undergoing a color change when combined with the Grubbs' catalyst. A difference was observed between these results and the reported color reaction that is supposed to take place instantaneously.<sup>3,4</sup> Over an hour passed before there was an indication of a change. This may be because the Grubbs' catalyst had a layer of wax protecting it and it took time for the COT to diffuse through the wax. Despite the longer than expected time period, the COT successfully underwent the color change reaction. This verifies that the wax protection is an effective method to prevent Grubb's catalyst deactivation from exposure to air while allowing it to retain functionality as catalyst for color changing reactions.

### **5.3 Production of Mechanical Testing Specimens**

The specimens used for the modified compact tension testing were prepared by curing the epoxy in a mold to produce a bar. The resultant epoxy bar was then machined into multiple modified compact tension specimens as described in Section 4.7. During the process of producing these specimens, differential scanning calorimetry (DSC) tests were performed to assess the properties of the specimens. Several observations of the specimen material were also noted during specimen production.

#### **5.3.1 Differential Scanning Calorimetry Results**

During preparation of the Cab-o-sil epoxy bar, a small sample of the uncured epoxy was collected and tested using a DSC. While collecting heat flow data, the sample was heated from ambient temperature to 250°C, then cooled to -50°C, then heated to 250°C once more, with heating and cooling rates of 10°C per minute. The results of this test were plotted and are shown in Figure 5.10.

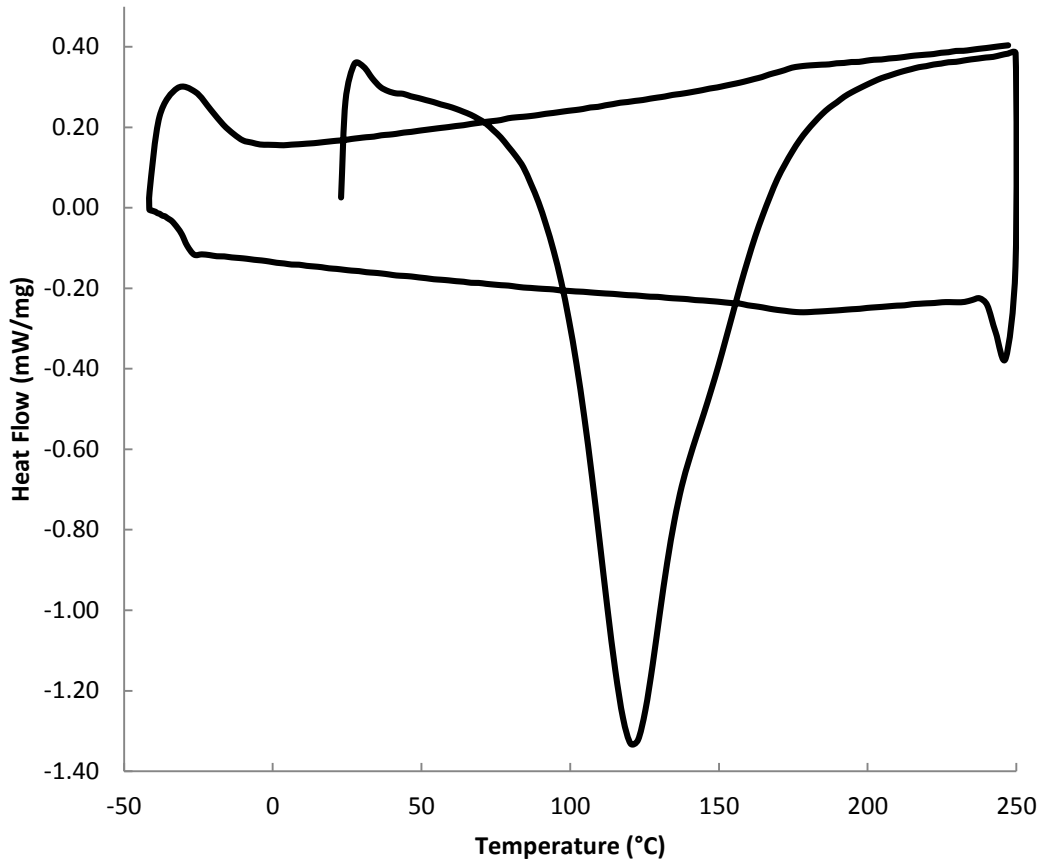


Figure 5.10: Uncured Epoxy DSC Test Results

The data was collected with endothermic flow in the positive direction and exothermic flow in the negative direction. The information that can be obtained from the DSC results is the glass transition temperature ( $T_g$ ) of the epoxy and the enthalpy of the curing reaction that took place as the uncured sample was heated. The peaks at  $-32^\circ\text{C}$  and  $31^\circ\text{C}$  and local minimum at  $246^\circ\text{C}$  were considered to be artifacts of the DSC testing process. The local minimum at  $121^\circ\text{C}$  however, was used to determine the enthalpy of the curing reaction by integrating the area under the peak in reference to a baseline.

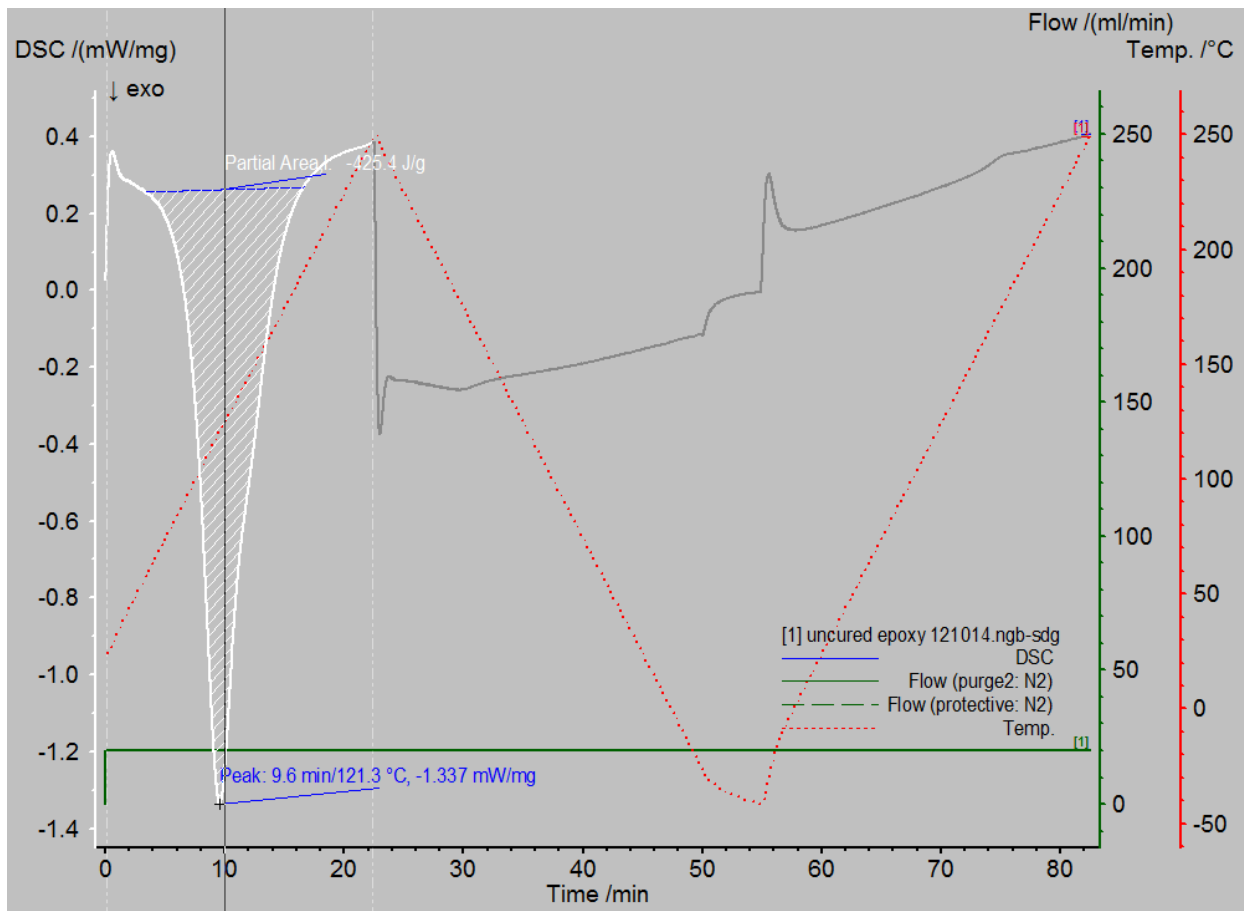


Figure 5.11: Determination of Enthalpy of Curing Reaction for Uncured Epoxy

The DCS Netzsch software was used to determine the enthalpy of reaction. The enthalpy is equal to the area under the peak relative to a base line, which is equal to the y-value at the point where the area is taken to start. The enthalpy of reaction was found to be -425 J/g.

The T<sub>g</sub> was determined by using the point of inflection on the near linear segment of the curve with time values between 70 and 80 minutes.

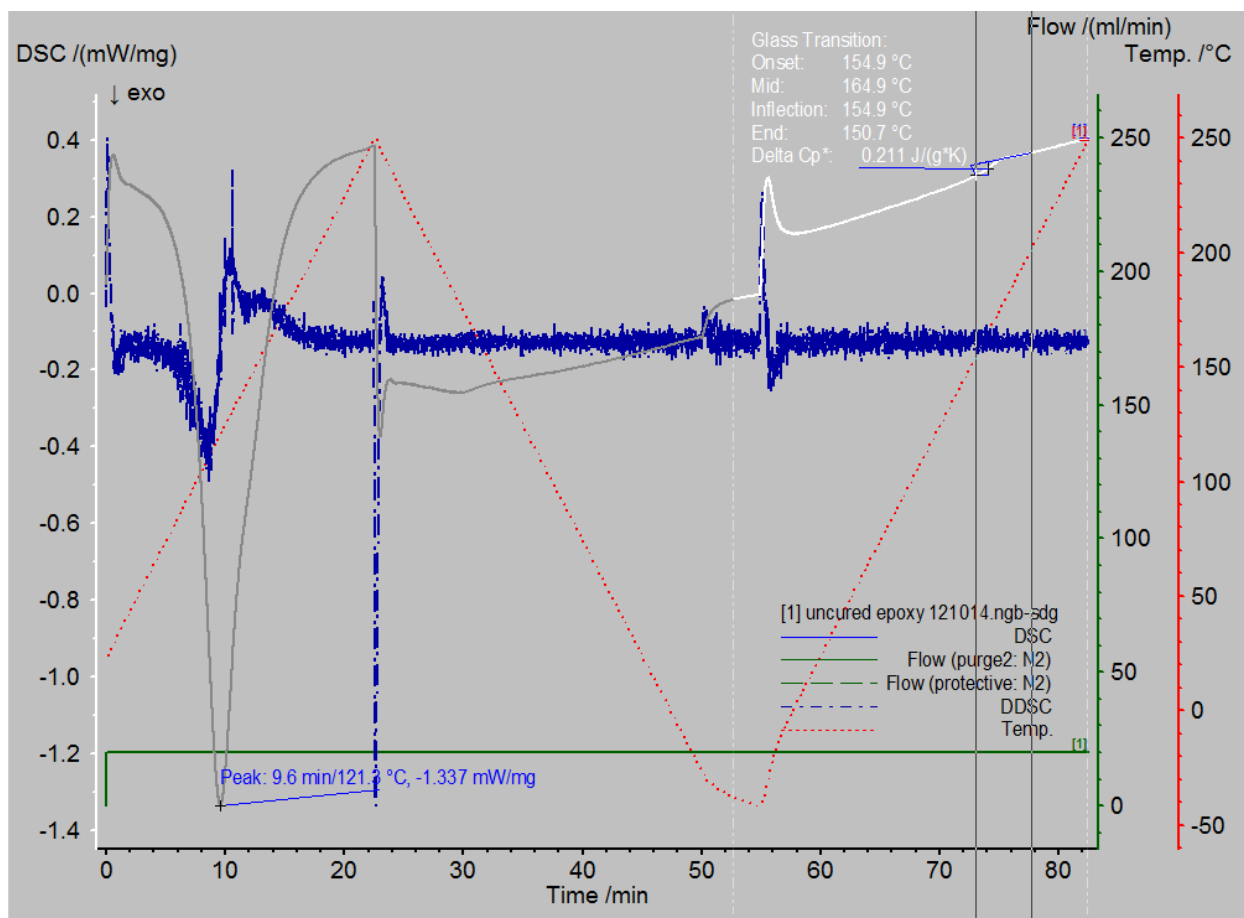


Figure 5.12: Determination of  $T_g$  for Uncured Epoxy

The DCS Netzsch software was used to determine the  $T_g$  of the epoxy, which was found to be 164.9°C. This value is consistent with the literature value for pure epoxy of 165°C.<sup>13</sup>

A similar DSC analysis was conducted for a small sample of the cured epoxy bar containing only Cab-o-sil. The epoxy bar was cured under the same conditions as the DCPD and DCPD-COT epoxy bars. Like the uncured epoxy sample, the sample was heated from ambient temperature to 250°C, then cooled to -50°C, then heated to 250°C once more, with heating and cooling rates of 10°C per minute. The results of this test are shown in Figure 5.13.



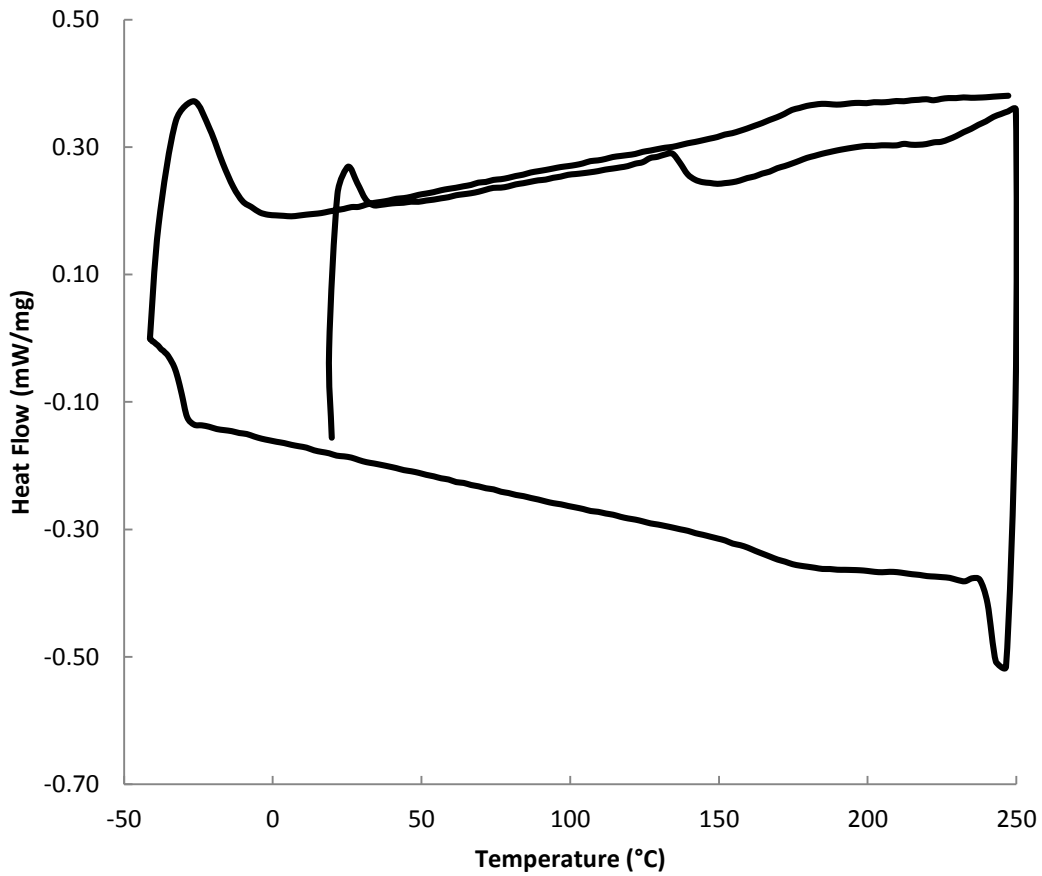


Figure 5.13: Cured Epoxy DSC Test Results

The peak that was used to determine the enthalpy of the curing reaction occurs at 149°C. This peak is much smaller than the peak of the uncured sample because the enthalpy of the curing reaction is much greater in the uncured sample, while the cured sample has already cured to a large extent before the DCS testing has taken place.

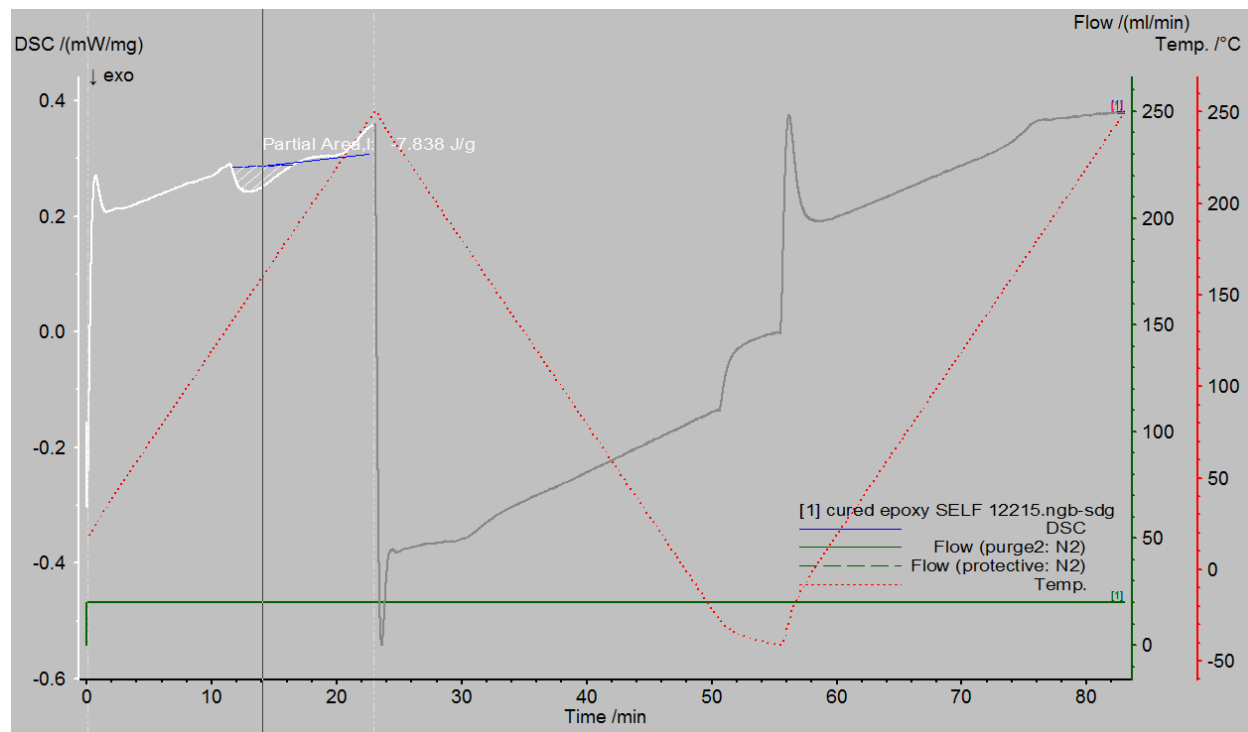


Figure 5.14: Determination of Enthalpy of the Curing Reaction for Cured Epoxy

The DCS Netzsch software was used to determine the enthalpy of reaction for the cure sample as well. The enthalpy of reaction was found to be  $-7.838 \text{ J/g}$ .

The glass transition temperature of this sample was determined by using the point of inflection on the near linear segment of the curve with time values between 70 and 80 minutes as well.

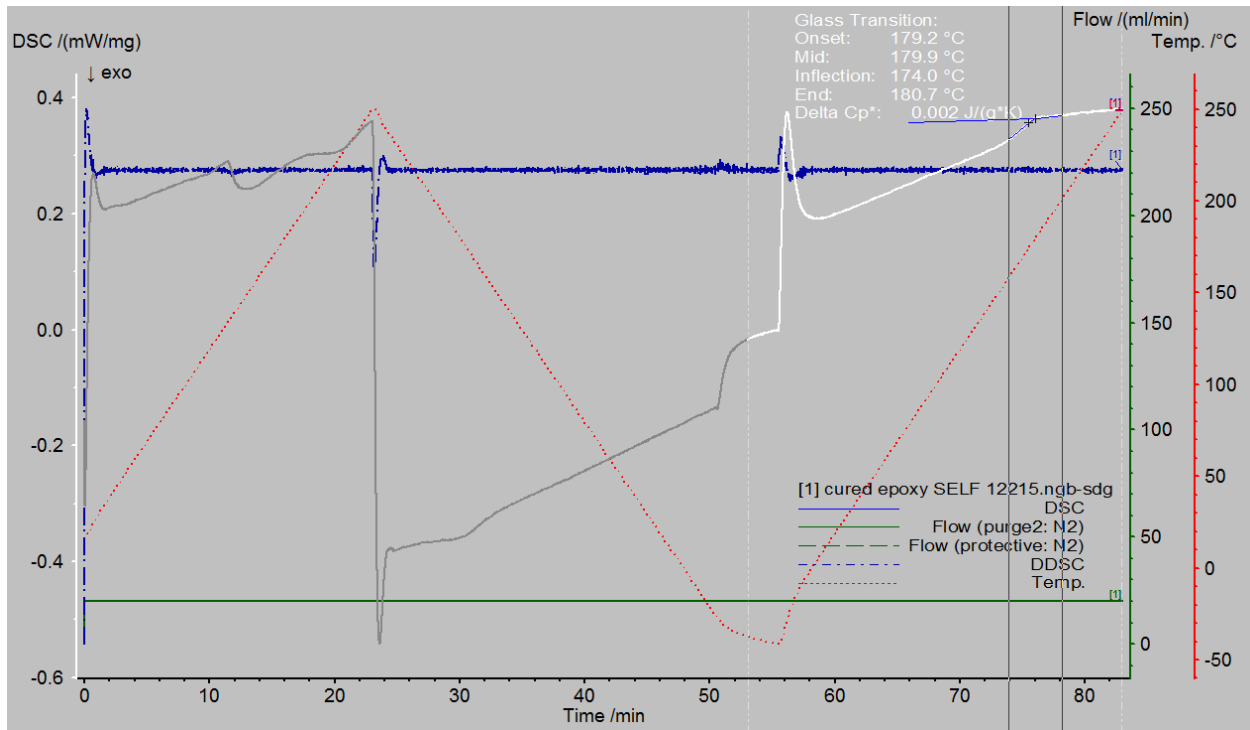


Figure 5.15: Determination of  $T_g$  for Cured Epoxy

The DCS Netzsch software was used to determine the glass transition temperature of the epoxy, which was found to be 179.9 °C. This value is higher than the value of the glass transition temperature found for the uncured epoxy sample and the literature value for pure epoxy of 165 °C.<sup>13</sup> This may be due to the fact that the sample had already been cured once, and curing it a second time could affect its properties including its glass transition temperature.

From the analysis of both the cured and uncured samples of the epoxy containing Cab-o-sil, it was possible to determine how cured the specimens used in the modified compact tension test were. The values of the enthalpy of reaction of both the uncured and cured samples were used to determine that the specimens used for the testing were 98.2 percent cured. Because the DCPD and DCPD-COT epoxy bars were cured under the same conditions as the Cab-o-sil epoxy bar, it can reasonably be assumed that the DCPD and DCPD-COT specimens were cured to a similar extent.

### 5.3.2 Microscope and SEM Images of the Specimens

Unusual voids were seen in the DPCD and DCPD-COT epoxy bars as well as the Cab-o-sil bar. Since the Cab-o-sil bar contained only the epoxy components and the Cab-o-sil, the voids in this are necessarily air bubbles. This was confirmed with SEM images, Figure 5.16 and Figure 5.17, and Zeiss optical microscope, Figure 5.18.

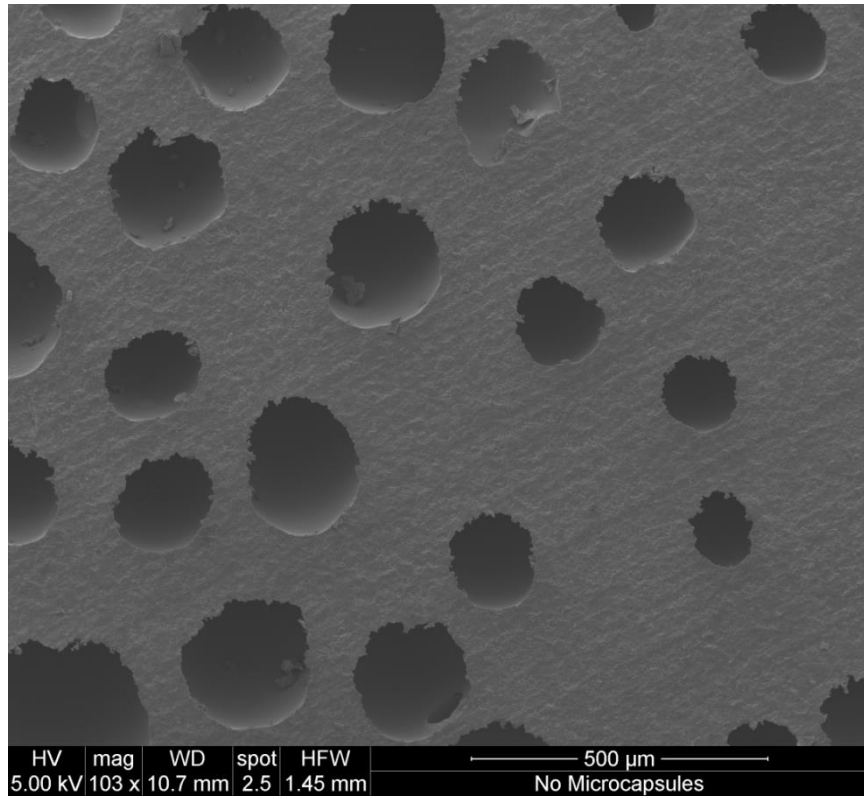


Figure 5.16: SEM Image of Cab-o-sil Surface

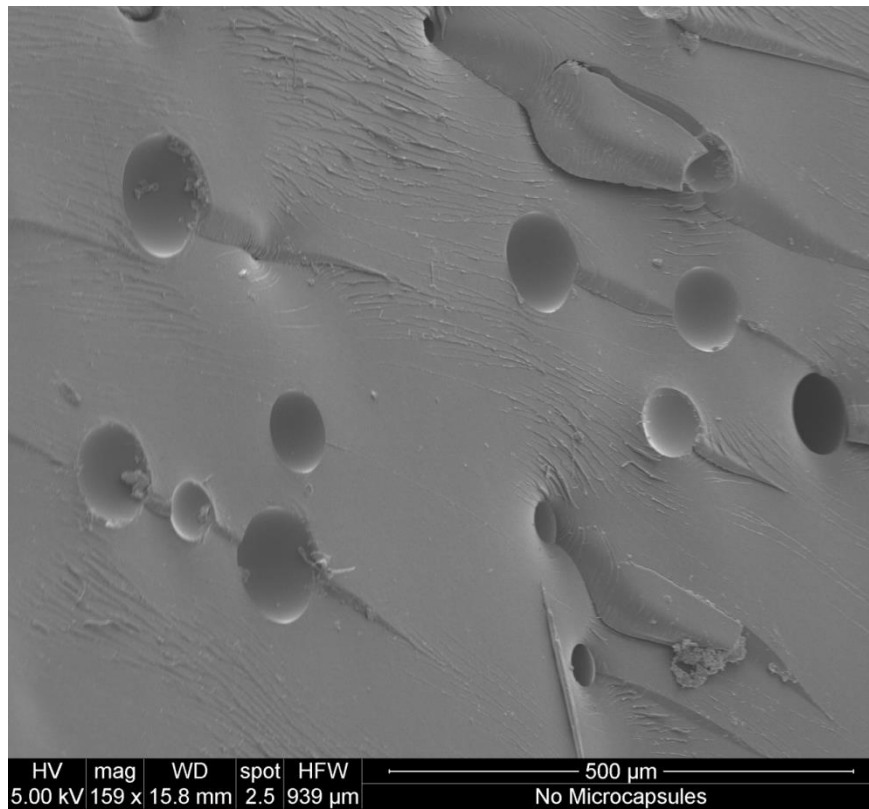


Figure 5.17: SEM Image of Cab-o-sil Surface

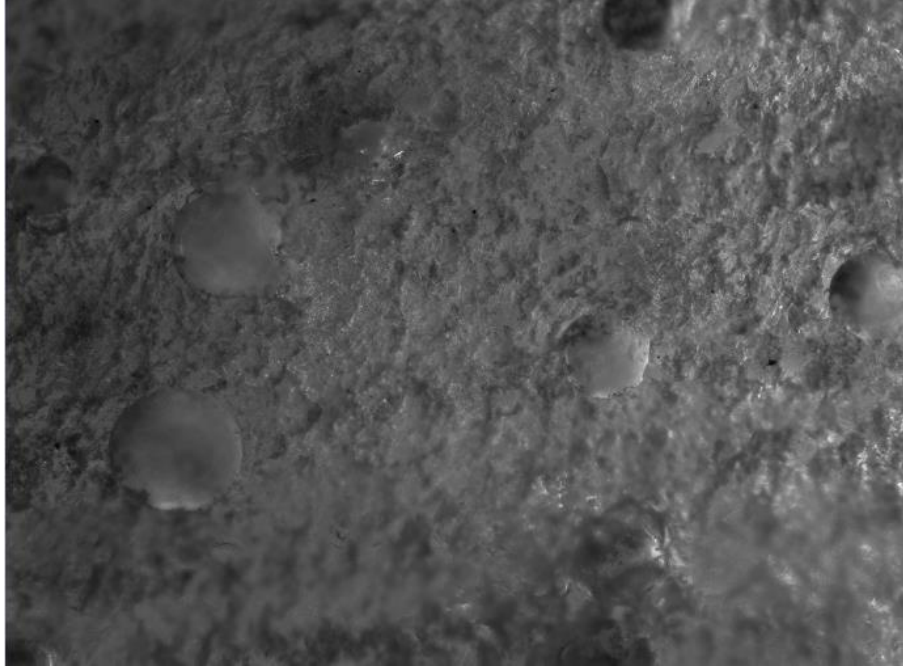


Figure 5.18: Optical Microscopy Image of Cab-o-sil Surface

These images provided a reference when looking at the DCPD and DCPD-COT epoxy bars. The crack edge can be seen by the Zeiss optical microscope, Figure 5.19, and the SEM images, Figure 5.20.

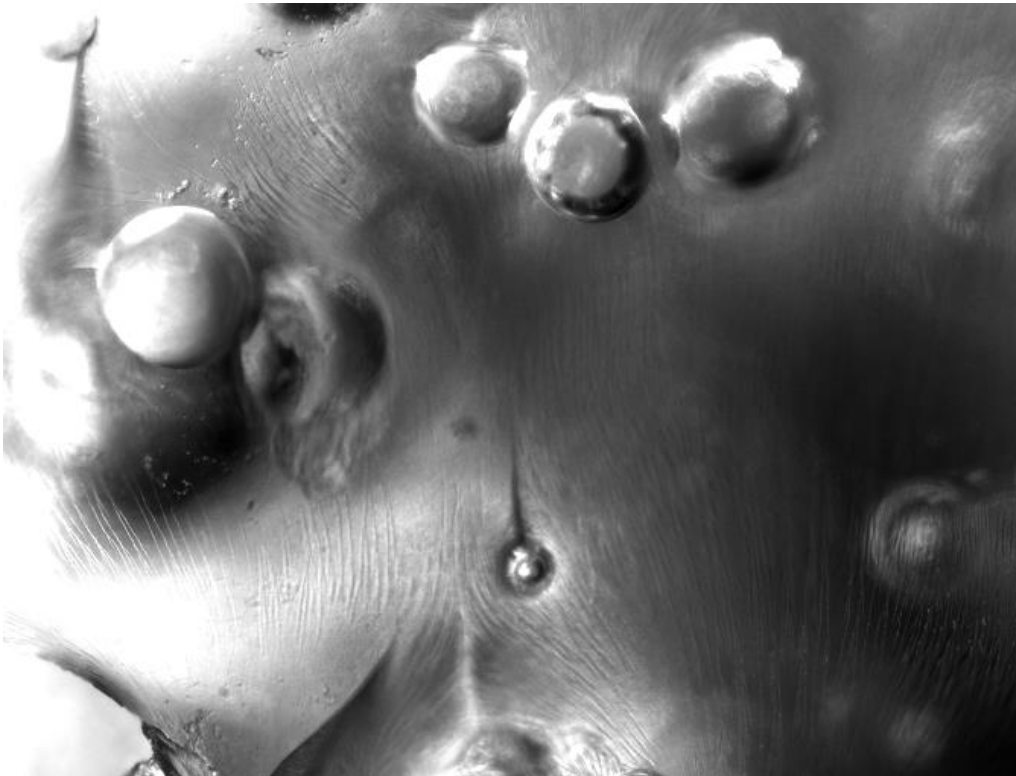


Figure 5.19: Voids and Microcapsules near DCPD Sample Crack Surface

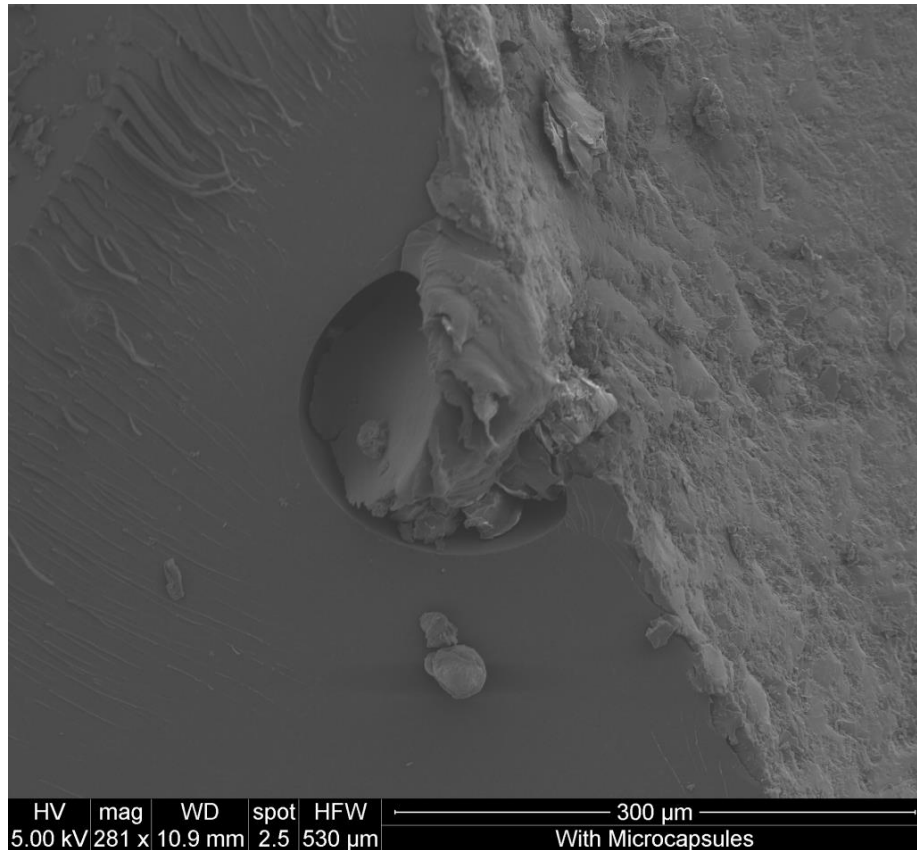


Figure 5.20: SEM Image of DCPD Crack Edge

A number of spheres approximately 50-200  $\mu\text{m}$  in size are visible near the crack surface in Figure 5.19. Based on Cab-o-sil bar figures, it is believed some of these spheres are air bubbles. However, it is certain that there were at least some microcapsules at the crack surface. It was initially believed that the crack pinning seen in image Figure 5.19 was from the microcapsules but the SEM image of the Cab-o-sil, Figure 5.17, also shows crack pinning characteristics.<sup>41</sup> Figure 5.20 on the other hand, provides a definite image of a microcapsule. It is clearly seen that the microcapsule has ruptured and polymerized at the crack surface.

### 5.3.3 Observations Made During Machining of the Specimens

During the production of the DCPD and DPCD-COT microcapsules, it was noted that DCPD and COT produced very strong odors that make the compounds easily identifiable. This strong smell is common among aromatic compounds. During the machining of the bars, it was noted that the characteristic odors of DCPD and COT were present. This indicates that microcapsules were being ruptured during the machining of the specimens. From this observation it can be concluded that at least some of the microcapsules had remained intact during the curing process.

Figure 5.21 shows a specimen of the DCPD bar that was prepared for the modified compact tension test labeled D5 (left), and a specimen of the DCPD-COT bar that was prepared for the

modified compact tension test labeled C6 (right). The large voids and dark spots that are possible indications of charring that occurred during the production of the epoxy bars can be seen in these samples.



Figure 5.21: Specimens D5 and C6 Before Testing

#### 5.4 Mechanical Testing

The modified compact tension specimens were tested on the Instron with a loading rate of 0.1 mm/min, while load and displacement were recorded. An example of the raw data generated this way can be seen in Figure 5.22.

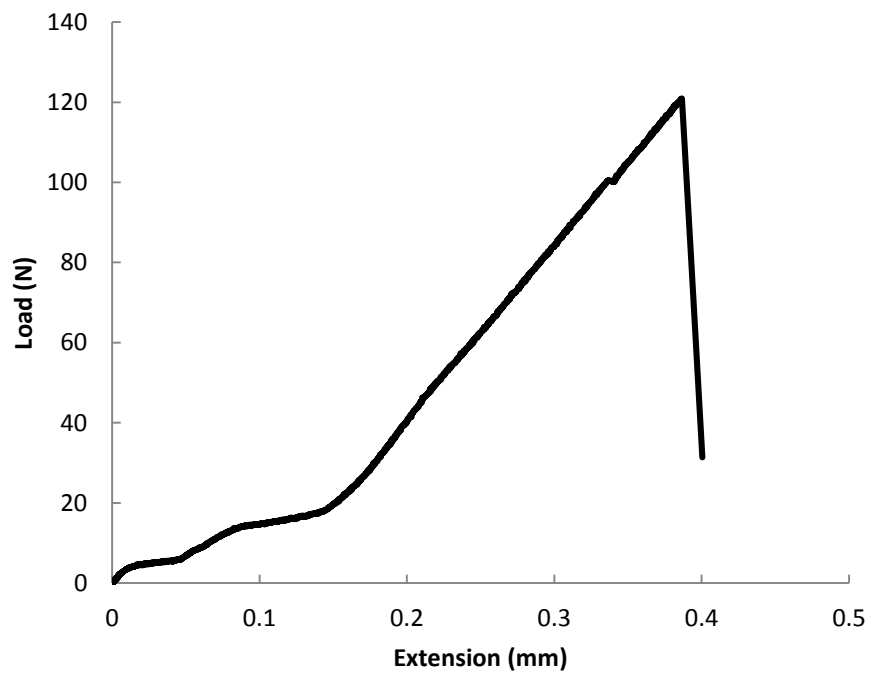


Figure 5.22: Loading of DCPD-COT Specimen

The breaking force of the specimens ranged from approximately 88-120 N or 9-12 kgf. The average breaking force the DCPD-COT specimens was  $102.9 \text{ N} \pm 12.0 \text{ N}$  and the average for the DCPD specimens was  $104.9 \text{ N} \pm 8.6 \text{ N}$ . Figure 5.23 displays the average standard deviation for each data set along with the minimum and maximum values obtained during testing. As was noted above, the bars had significant voids in them so it is unknown how they would have performed without such voids. From these results it can be concluded that the DCPD-COT and DCPD specimens showed no significant difference in breaking strength, meaning the addition of COT did not detract from the breaking strength of the specimens.

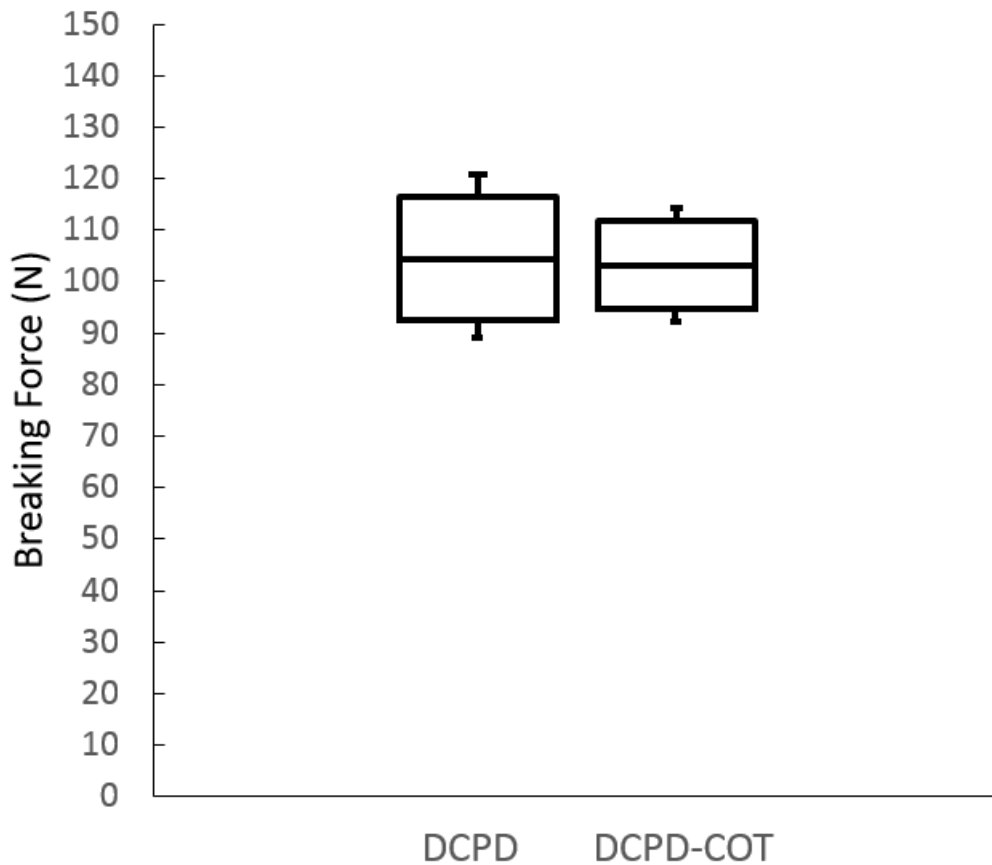


Figure 5.23: Breaking Force of Modified Compact Tension Specimens

The specimens broke into two pieces because the crack did not stop at the arresting hole. The two pieces of the specimens were placed together and allowed to heal for twenty-four hours under an aluminum plate to create low pressure healing conditions, 0.018 MPa.<sup>14</sup> When checked after the twenty-four hours, the specimens could not be picked up as a single piece. The specimens did not heal along the crack. No color difference was seen after the twenty-four hour healing period either.



Obstacles inhibiting sample healing include non-uniform dispersion and the presence of voids. Both of these obstacles are characteristics that limit the proximity of the Grubbs' catalyst and microcapsules within the epoxy, making it less likely for self-healing mechanisms to occur. Non-uniform dispersion and voids were most likely caused during the production of epoxy bars.

Non-uniform dispersion results in segregation of microcapsules and the Grubbs' catalyst. Both components of the self-healing system need to be in proximity with each other for the desired reaction to occur. Dispersion is heavily influenced by the mixing cycle used to make epoxy bars, so there should be an ideal mixing rate that is acceptable for this purpose. Under mixing causes the components in the mixture to be inhomogeneously dispersed throughout the epoxy. Over mixing increases the chance that a significant portion of the microcapsules will rupture during the mixing cycle. After mixing in all the components for the production of these bars, viscosities increased noticeably. This increased viscosity may have made it more difficult for microcapsules to disperse across the epoxy mixture resulting in a gradient of microcapsule concentration.

It is known through SEM imaging, Figure 5.20, that some polymerization occurred at the crack surface. However, the specimens failed to heal. This could have been due to a lack of components on the crack edge. Even if microcapsules were successfully dispersed throughout the epoxy there might not have been enough microcapsules to promote significant healing at damage sites to occur if too many of them ruptured during mixing. There were 3.7 g microcapsule and 10.1 g protected Grubbs' catalyst per 100 mL epoxy. The ratio of microcapsule to epoxy and Grubbs' catalyst to microcapsules fell within the optimal range of Brown et al.'s research on microcapsule and catalyst loading.<sup>39</sup> The Grubbs' protection procedure may have also contributed to not having enough of the active components on the crack edge. Healing agents within the microcapsules have less access to the Grubbs' catalyst after the Grubbs' catalyst is coated in wax. There should be an ideal ratio of wax relative to Grubbs' catalyst that should be introduced in the system which adequately protects the Grubbs' catalyst but does not present too much of a barrier for diffusion of healing agents. However, this ratio of wax is not known and any Grubbs' catalyst at the crack edge may not have been active enough for healing to occur.

The large voids could have prevented contact of the microcapsules and the Grubbs' catalyst, therefore averting healing. It is believed that the voids seen in the DCPD and DCPD-COT epoxy bars are pockets of conglomerated air bubbles which were observed in the Cab-o-sil bar, see Section 5.3.2. The Cab-o-sil was added to the epoxy to act as a thixotropic agent, which enables even dispersion of the components. However, it is now thought that the Cab-o-sil increased the viscosity of the epoxy too much and prevented air bubbles from escaping during the thirty second de-foaming step after being mixed in. When the components of the DCPD and DCPD-COT bars were then mixed in at a slower mixing rate to prevent microcapsule rupture, the air bubbles in the epoxy mixture conglomerated to form the large voids. In addition to having an impact on the healing, these large voids also potentially had an impact on the mechanical properties of the specimen.

## 6.0 Conclusions and Recommendations

### 6.1 Conclusions

Microcapsules were successfully created containing both a healing agent, DCPD, and a damage detection agent, COT. When these microcapsules were ruptured in the presence of the Grubbs' catalyst, a color change was observed. Because the color change test was successful, it can be concluded that DCPD-COT microcapsules could be used in place of DCPD microcapsules in a self-healing polymer to provide damage detection.

DCPD microcapsules were added to epoxy in a ratio of 3.7 g microcapsules per 100 mL of epoxy, which was then machined to produce modified compact tension specimens. DCPD-COT specimens were produced in this way as well. The results of the mechanical testing showed that the average breaking force of the DCPD modified compact tension specimens tested is  $104.9 \text{ N} \pm 8.6 \text{ N}$ . The average breaking force of the DCPD-COT modified compact tension specimens is  $102.9 \text{ N} \pm 12.0 \text{ N}$ . It can be concluded that the breaking force of the specimens tested was not significantly affected by replacing DCPD microcapsules with DCPD-COT microcapsules. This suggests that DCPD-COT microcapsules could be incorporated into a self-healing polymer in place of DCPD microcapsules for the purpose of damage detection without significantly affecting the polymer's breaking strength.

No conclusion can be made about the effect of using DCPD-COT microcapsules in place of DCPD microcapsules on the specimens' healing efficiencies. This is because after testing the DCPD and DCPD-COT modified compact tension specimens to determine their breaking forces, the specimens were given 24 hours to heal. The specimens failed to heal during this time period, and their healing efficiencies could not be tested.

### 6.2 Recommendations

Some recommendations are provided based on the experience gained by working on this project. First, it is recommended that the Grubbs-Love catalyst be used for better contrast. Despite the small amount of Grubbs' catalyst that was used in the epoxy specimens, 0.4 g unprotected per 100 mL epoxy, the distinct red color of the Grubbs' catalyst was clearly present throughout the specimen. The COT-Grubbs' catalyst reaction also creates a red-purple color after long term polymerization. Therefore, it is suggested that the Grubbs-Love catalyst be used, which is nearly colorless, so that this reaction can be seen more clearly.

It is also recommended that more testing be conducted on the need for a thixotropic agent. This testing should assess if the curing of the epoxy resin with the amine curing agent is fast enough that a thixotropic agent is not needed. It was observed that the addition of Cab-o-sil to the epoxy mixture caused small air bubbles, which developed into large voids when more components were added. If a thixotropic agent is needed, an agent other than Cab-o-sil should be picked. Alternatively, a different mixing order or different mixing times/rates may be more effective.

The final recommendation is that more testing should be conducted on the amount of microcapsules needed for a significant reaction with the Grubbs' catalyst. It is possible healing was not able to occur because of a lack of microcapsules to react with the Grubbs' catalyst. More

testing should be easy to conduct with DCPD-COT microcapsules, since the reaction can be seen visually.

## Appendix

### Appendix A: Microencapsulation Procedure

Adapted from the procedure of Brown et al.<sup>10</sup>

Microcapsules were prepared using an oil-in-water emulsion. A 500 mL beaker was placed in a temperature controlled water bath. At room temperature, 100 mL of deionized water and 25 mL of 2.5 wt% aqueous solution of EMA copolymer were added and stirred with a mechanical stirrer at 550 rpm. Under agitation, 2.50 g urea, 0.25 g ammonium chloride, and 0.25 g resorcinol were added to the solution. The pH was raised from approximately 2.6 to 3.5 by drop-wise addition of sodium hydroxide. One drop of 1-octanol was added to eliminate bubbles. Slowly, 30 ml of DCPD was added and allowed to stabilize for 10 minutes. After 10 minutes, 6.33 g of 37 wt% aqueous solution of formaldehyde was added. The emulsion was covered with aluminum foil and heated to 55°C. After four hours of continuous stirring, the mixer and hot plate were switched off. The suspension of microcapsules was separated under vacuum with a coarse filter. The microcapsules were rinsed with deionized water and air dried for 24-48 h.

### Appendix B: Grubbs' Protection Procedure

Adapted from the procedure of Rule et al.<sup>21</sup>

Grubbs' catalyst is very sensitive to air. Therefore, it needs to be protected before adding it to an epoxy system. This can be done by encapsulating it in paraffin wax. In an N<sub>2</sub>-filled glove box, the 0.5 grams Grubbs' catalyst is added to a vial with 9.6 grams paraffin wax. An emulsion was prepared in 1000 mL beaker with 225 mL of water, 0.63 g poly(ethylene-*co*-maleic anhydride) (EMA copolymer), and one drop of 1-octanol. The emulsion was placed in an 82 °C water bath and stirred with a mechanical stirrer at 900 rpm. The vial containing the wax and the catalyst was submerged in the same 82 °C water bath. Once the wax was melted, approximately 10 minutes, it was shaken and poured into the emulsion. After 2 min, cold water (600 mL cooled in the refrigerator) was quickly added, and the stirring was stopped. The microspheres were collected by filtration and dried in the vacuum oven at room temperature.

## References

---

- <sup>1</sup> Wu, D. Y.; Meure, S.; Solomon, D. Self-healing polymeric materials. *Prog. Polym. Sci.* **2008**, *33*, 479–522.
- <sup>2</sup> Pang, J.; Bond, I. P. A hollow fibre encompassing self-healing and enhanced damage visibility. *Compos. Sci. Technol.* **2005**, *65*, 1791-1799.
- <sup>3</sup> Odom, S. A.; Jackson, A. C.; Prokup, A. M.; Chayanupatkul, S.; Sottos, N. R.; Moore, J. S. Visual Indication of Mechanical Damage Using Core–Shell Microcapsules. *ACS Appl. Mater. Interfaces* **2011**, *3*, 4547–4551
- <sup>4</sup> Odom, S. A., Caruso, M. M., Finke, A. D., Jackson, A. C., Moore, J. S., Sottos, N. R., & White, S. R. System for visual indication of mechanical damage. U.S. Patent 8,846,404, September 30, 2014.
- <sup>5</sup> Blaiszik, B. J.; Kramer, S. L. B.; Olugebefola, S. C.; Moore, J. S.; Sottos, N. R.; White, S. R. Self-Healing Polymers and Composites. *Materials Research* **2010**. 179-211.
- <sup>6</sup> Zhang, M. Q.; Rong, M. Z Self- Healing Polymers and Polymer Composites, *EngineeringPro* **2011**.
- <sup>7</sup> Toohey, K. S.; Hansen, C. J.; Lewis, J. A.; White, S. R., Sottos, N. R. Delivery of Two- Part Self-Healing Chemistry via Microvascular Networks. *Advanced Functional Materials* **2009**.
- <sup>8</sup> Hayes, S. A.; Zhang, W.; Branthwaite, M.; Jones, F.R. Self-healing of damage in fiber-reinforced polymer-matrix composites. *J. R. Soc. Interface.* **2001** *4*, 381-387
- <sup>9</sup> Bergman, S. D.; Wudl, F.; Mendable Polymers. *J. Mater. Chem.*, **2008**,**18**, 41-62
- <sup>10</sup> Brown, E. N.; Kessler, M. R.; Sottos, N. R.; White, S. R. In situ poly(urea-formaldehyde) microencapsulation of dicyclopentadiene. *Journal of Microencapsulation* **2003**.
- <sup>11</sup> Rochmadi; Prasetya A.; Hasokowati W. Mechanism of Microencapsulation with Urea-Formaldehyde Polymer. *American Journal of Applied Sciences* **2010**, *739-745*, 1546-9239.
- <sup>12</sup> White, S. R.; Sottos, N. R.; Geubelle, P. H.; Moore, J. S.; Kessler, M. R.; Sriram, S. R.; Brown, E. N.; Viswanathan, S. Autonomic healing of polymer composites. *Nature* **2001**, 794-797.
- <sup>13</sup> Park, E.; Park, J.; Jeon, J.; Sung, J.; Hwang, W.; Lee, B. Ring-opening metathesis polymerization of dicyclopentadiene and tricyclopentadiene. *Macromolecular Research* **2012**.

- 
- <sup>14</sup> Rahmathullah, M.; Palmese, G. Crack-Healing Behavior of Epoxy–Amine Thermosets. *Journal of Applied Polymer Science* **2009**, 113, 2191–2201.
- <sup>15</sup> Dorworth, L. Proceedings from SAMPE '09: Society for Advancement on Materials and Process Engineering Conference. Baltimore, 2009.
- <sup>16</sup> Grubbs, R. H. Olefin Metathesis. *Tetrahedron* **2004**, 7117-7140, 0040-4020.
- <sup>17</sup> Schubert, U. *Advances in Metal Carbene Chemistry*, NATO ASI Series, 1989.
- <sup>18</sup> Leitgeb, A.; Wappel, J.; Slugovc, C. The ROMP toolbox upgraded. *Polymer* **2010**, 2927-2946, 0032-3861.
- <sup>19</sup> Blaiszik, B.J.; Sottos, N.R.; White, S.R. Nanocapsules for self-healing materials. *Composites Science and Technology* **2008**, 978-986, 0266-3538.
- <sup>20</sup> Rochmadi; Prasetya A.; Hasokowati W. Mechanism of Microencapsulation with Urea-Formaldehyde Polymer. *American Journal of Applied Sciences* **2010**, 739-745, 1546-9239.
- <sup>21</sup> Rule, J. D., Brown, E. N., Sottos, N. R., White, S. R., & Moore, J. S. Wax-Protected Catalyst Microspheres for Efficient Self-Healing Materials. *Advanced Materials* **2005**, 17, 205-208.
- <sup>22</sup> Pham, H. Q.; Marks, M. J. Epoxy Resins. *Kirk-Othmer Encyclopedia of Chemical Technology*, 2004.
- <sup>23</sup> Ratna, D. *Handbook of Thermoset Resins*, Smithers Rapra Technology, 2009.
- <sup>24</sup> Lee, J. K.; Hong, S. J.; Liu, X.; Yoon, S. H. Characterization of dicyclopentadiene and 5-ethylidene-2-norbornene as self-healing agents. *Macromolecular Research* **2004**, 10, 478-483.
- <sup>25</sup> Noh, H.H.; Lee, J.K. Microencapsulation of self-healing agents containing a fluorescent dye. **2012**, 9.
- <sup>26</sup> Toohey, K. S.; Hansen, C. J.; Lewis, J. A.; White S. R.; Sottos N. R. Delivery of Two-Part Self-Healing Chemistry via Microvascular Networks. *Advanced Functional Materials* **2009**, 19, 1339-1405.
- <sup>27</sup> Li, H.; Wang, R.; Liu, W. Surface modification of self-healing poly(urea-formaldehyde) microcapsules using silane-coupling agent. *Applied Surface Science* 2008, 255, 1894–1900.
- <sup>28</sup> Bains, G. K.; Kim, S. H.; Sorin, E. J.; Narayanaswami, V. The Extent of Pyrene Excimer Fluorescence Emission Is a Reflector of Distance and Flexibility. *Am. Chem. Soc.* 2012, **51**, 6207–6219.
- <sup>29</sup> Turro, N. J.; Arora, K. S.; Pyrene as a photophysical probe for intermolecular interactions. *Polymer* **1986**, 27.

- 
- <sup>30</sup> Bogan, G.W; The Dow Chemical Company. Unique polyaromatic cyanate ester for low dielectric printed circuit boards. *SAMPE Journal* **1988**; 24 (6): 19-25.
- <sup>31</sup> Liaw, D. Pyrene-containing norbornene methylene amine and polymer thereof, and method for manufacturing the polymer. **2011**, 113.
- <sup>32</sup> Jimenez, I. Y.; Bartha, R. Solvent-Augmented Mineralization of Pyrene. *Appl. Environ. Microbiol.* **1996**, 62, 2311-2316.
- <sup>33</sup> McIlroy, D. A.; Blaiszik, B. J.; Caruso, M. M.; White, S. R.; Moore, J. S.; Sottos, N. R. Microencapsulation of a Reactive Liquid-Phase Amine for Self-Healing Epoxy Composites. *Macromolecules* **2010**, 43, 1855–1859.
- <sup>34</sup> Bleay, S. M.; Loader, C. B.; Hawyes, V. J.; Humberstone, L.; Curtis, P. T. A smart repair system for polymer matrix composites. *Composites, Part A* **2001**, 31, 1767-1776.
- <sup>35</sup> Klinga, S.; Czigány, T. Damage detection and self-repair in hollow glass fiber epoxy composite. *Compos. Sci. Technol.* **2014**, 99, 82-88.
- <sup>36</sup> Bruns, N.; Pustelny, K.; Bergeron, L. M.; Whitehead, T. A.; Clark, D. S. Mechanical Nanosensor Based on FRET within a Thermosome. *Angew. Chem., Int. Ed.* **2009**, 48, 5666-5669.
- <sup>37</sup> Makyła, K.; Müller, C.; Lörcher, S.; Winkler, T.; Nussbaumer, M. G.; Eder, M.; Bruns, N. Fluorescent Protein Senses and Reports Mechanical Damage. *Advanced Materials* **2013**, 25, 2701-2706.
- <sup>38</sup> Löwe, C.; Weder, C. Excimers as Molecular Probes: Deformation-Induced Color Changes. *Advanced Materials* **2002**, 14, 1625-1629.
- <sup>39</sup> Brown, E. N.; Sottos, N. R.; White, S. R. Fracture testing of a self-healing polymer composite. *Experimental Mechanics* **2002**, 42, 372-379
- <sup>40</sup> Dicyclopentadiene ; MSDS No. AC150760000 [Online]; Fisher Scientific: Fair Lawn, NJ , May 20, 2010. (accessed Feb 11, 2015).
- <sup>41</sup> Chaudhary, S., Parthasarathy, S., Kumar, D., Rajagopal, C., & Roy, P. Simple toughening of epoxy thermosets by preformed thermoplastics. *Society of Plastics Engineers* **2014**.